# Discovery of phenylselenoether-hydantoin hybrids as ABCB1 efflux pump modulating agents with cytotoxic and antiproliferative actions in resistant T-lymphoma

Wesam Ali[a,b], Gabriella Spengler[c], Annamária Kincses[c], Márta Nové[c], Cecilia Battistelli[d], Gniewomir Latacz[a], Małgorzata Starek[e], Monika Dąbrowska[e], Ewelina Honkisz-Orzechowska[a], Annalisa Romanelli[f], Manuela Monica Rasile[f], Ewa Szymańska[a], Claus Jacob[b]\*, Clemens Zwergel,[b,f,g]\* Jadwiga Handzlik[a]\*

*[a] Department of Technology and Biotechnology of Drugs, Jagiellonian University, Medical College, Medyczna 9, PL 30-688 Kraków, Poland*

*[b]Division of Bioorganic Chemistry, School of Pharmacy, Saarland University, Campus B 2.1, D-66123 Saarbruecken, Germany*

*[c] Institute of Medical Microbiology and Immunobiology, Faculty of Medicine, University of Szeged, Dóm tér 10, H-6720 Szeged, Hungary*

*[d] Istituto Pasteur Italia, Fondazione Cenci-Bolognetti, Department of Molecular Medicine, Sapienza University of Rome, Viale Regina Elena 324, 00161, Rome, Italy.*

*[e] Department of Inorganic Chemistry, Jagiellonian University, Medical College, Medyczna 9, PL 30-688 Cracow, Poland*
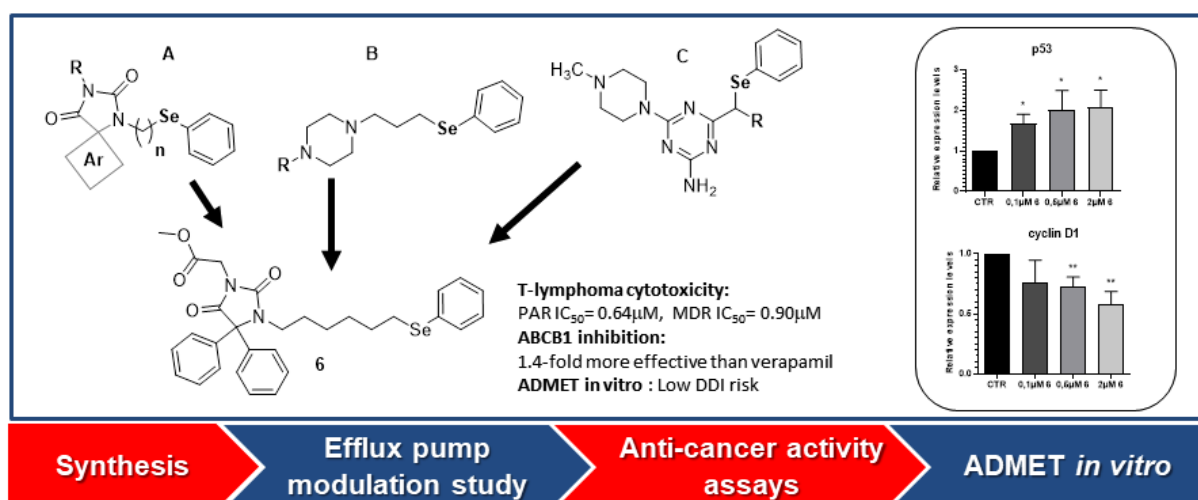
*[f] Department of Drug Chemistry and Technologies, Sapienza University of Rome, Piazzale Aldo Moro 5, 00185 Rome, Italy*

*[g] Department of Precision Medicine, "Luigi Vanvitelli" University of Campania, Via L. De Crecchio 7, 80138 Naples, Italy.*

\* Corresponding authors:

(J. Handzlik) E-mail address: j.handzlik@uj.edu.pl; (C. Jacob) E-mail address: c.jacob@mx.uni-saarland.de;(C. Zwergel) E-mail address: clemens.zwergel@uniroma1.it

**Graphical Abstract**



T-lymphoma cytotoxicity:
PAR $IC_{50}$= 0.64μM, MDR $IC_{50}$= 0.90μM
**ABCB1 inhibition:**
1.4-fold more effective than verapamil
**ADMET in vitro :** Low DDI risk

Synthesis → Efflux pump modulation study → Anti-cancer activity assays → ADMET *in vitro*

**Research Highlights:**

- Design and synthesis of new phenyl selenium ether hybrids.

- ABCB1 efflux pump modulating assays in mouse T-lymphoma cancer cells.

- Cytotoxic and anti-proliferative activity assays in sensitive and MDR cancer cells

- Effects on proliferation rate and cell cycle in human JURKAT cancer T-cells

- ADME-Tox profile *in vitro* for most active agents investigated

## Abstract

Multidrug resistance (MDR) in cancer cells is a crucial aspect to consider for a successful cancer therapy. P-gp/ABCB1, a member of ABC transporters, is involved in the main tumour MDR mechanism, responsible for the efflux of drugs and cytotoxic substances. Herein, we describe a discovery of potent selenium-containing ABCB1 MDR efflux pump modulators with promising anticancer activity. On three groups of selenoethers comprehensive studies in terms of design, synthesis, and biological assays, including an insight into cellular mechanisms of anticancer action as well as an ADMET-screening *in vitro* were performed, followed by in-depth SAR analysis. Among the investigated new phenylselenoether hybrids, four compounds showed significant cytotoxic and anti-proliferative effects, in particular, in resistant cancer cells. Hydantoin derivatives (**5**-**7**) were significantly more effective than the reference inhibitor verapamil (up to 2.6-fold at a 10-fold lower concentration) modulating ABCB1-efflux pump, also possessing a good drug-drug interaction profile. The best compound (**6**) was further evaluated in human JURKAT T-lymphocytic cancer cells for its impact on cell proliferation rate. Mechanistically, the expression of cyclin D1, an enhancer of the cell cycle, decreases, while p53, an inhibitor of cell proliferation, was up-regulated upon the treatment with compound **6** alone or in combination with the chemotherapeutic agent doxorubicin. In summary, a new chemical space of highly active selenium-containing anticancer agents has been discovered, with a new lead compound **6** that warrants more in-depth biological evaluation and further pharmacomodulation.

*Keywords:* MDR; selenother; ABCB1, P-glycoprotein inhibitor, T-lymphoma, JURKAT

# 1. Introduction

During the last decades, numerous new classes of anti-cancer drugs emerged, which usually support the natural body defence. At the same time, the cancer cells developed different mechanisms to face the cytotoxic effect of these drugs. In this field, the term of multidrug resistance (MDR) is defined as the low sensitivity for certain cells against drugs, often found in cancer for tumour therapy [1-5]. MDR is now a deeply investigated issue in the field of chemotherapy. It can result in the upregulation of drug efflux/ drug efflux pumps, cell growth, and survival signalling. MDR can also be related to the down-regulation of apoptosis signals or drug uptakes.
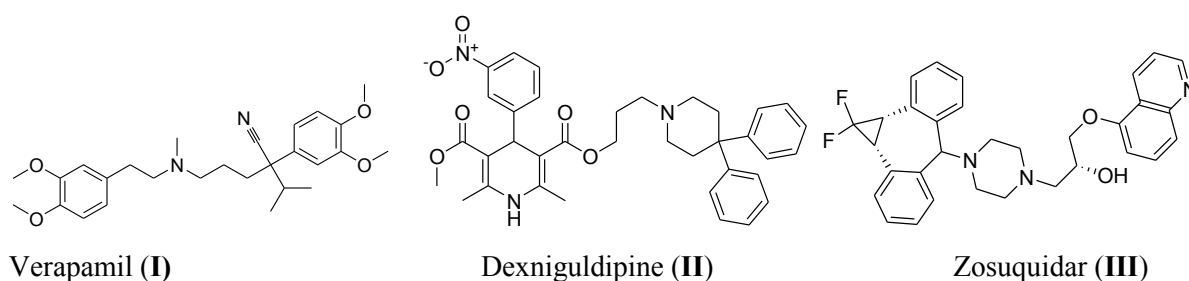
Nevertheless, key players of the MDR action are ATP-binding cassette (ABC) transporters, such as the P-glycoprotein (Pgp, ABCB1), MRP1 (ABCC1) and BCRP (ABCG2) ones [6], which are involved in essential processes in cancer cells' defence. Moreover, the inhibition of these transporters could be beneficial to overcome drug resistance [7]. In more detail, P-glycoprotein/ ABCB1 (P-gp/ABCB1) is a member of the ABC transporter family, which is encoded by the *MDR1* (*ABCB1*) gene, found in a plethora of healthy and cancerous cells. In the latter ones, they are often overexpressed and work as a self-defence against cytotoxic substances [8, 9] by acting as an efflux pump for various drugs, including anticancer agents.

One critical key in the battle against cancer is to overcome drug resistance thus to resume the activity of current or well-known anti-cancer drugs, *e.g.* topotecan, doxorubicin, vincristine, cisplatin, cyclophosphamide, methotrexate or 5-fluorouracil. A successful and well-accepted method in this field is the inhibition of P-gp function during chemotherapy [10]. The co-administration of efflux pump inhibitors (EPIs), which are specific compounds able to modulate the efflux action of MDR drug transporters, has been reported and well-reviewed [1-5]. Due to the complexity of cancer aetiology, a combined approach targeting these MDR proteins as well as hitting known antitumoral pathways such as p53 is more and more considered to be a successful strategy to fight cancer.
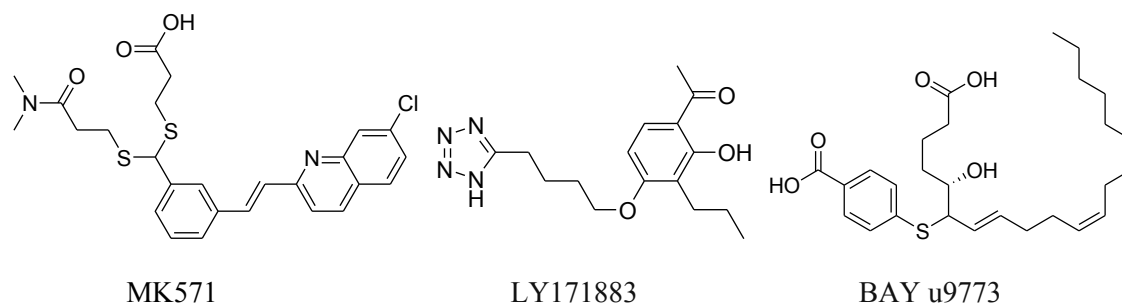
Recently, plenty of compounds that modulate P-gp in various assays conditions were synthesized and studied. Mainly, three generations of reversal MDR agents, *e.g.* verapamil (I), dexniguldipine (II) and zosuquidar (III) (Fig. 1A) have been widely investigated [1, 3, 7, 11]. Furthermore, a group of inhibitors for other ABC family members involved in cancer MDR, *i.e.* MRP1 (MK571, LY171883 and BAYu9773, Fig. 1B) and BCRP (Ko143 and FTC, Fig.

1C), have been evaluated [6]. However, their therapeutic usage is restricted by insufficient pharmaceutical profile, in particular, in the field of safety. Thus, further search for EPIs among new chemical groups is in great medical importance, but it is worth tu emphasize that rational design of new EPIs is a high challenge. Although recent scientific achievements provided crystal structures of some MDR ABC transporters,  the computer aided structure-based design is significantly limited in this protein family due to a variety of key-points that could be targeted by inhibiotors, and thus providing various structurally different "binding pockets". For instance, some structures can inactivate pump as enrgy users acting on ATP, while different structures can act via a competition with a drug-substrate to one of the binding sites.

(A)

Verapamil (**I**)          Dexniguldipine (**II**)          Zosuquidar (**III**)

(B)

MK571                LY171883                BAY u9773

(C)

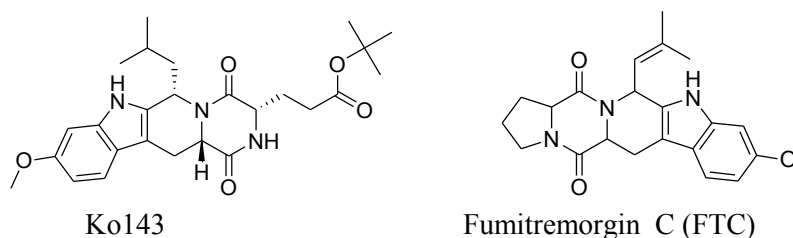Ko143                Fumitremorgin  C (FTC)

**Fig. 1.** Selected structures of cancer efflux ABC efflux pump inhibitors; (A) three generations (I-III) of ABCB1 inhibitors; (B) inhibitors of MRP1: MK571, LY171883 and BAYu9773; (C) inhibitors of BCRP: Ko143 and FTC [6].

On the other hand, the structure-activity relationship analysis (SAR) in the vast group of Pgp-modulators allowed to indicate a beneficial role for hydrophobic/aromatic ending

within their structures and also some flexibility in the middle (Fig. 1 A). Although the number of modulators found for either MRP1 or BCRP is much smaller, SAR for their several agents shows that both groups differ from the Pgp pharmacophores. In contrast to bulky aromatic ends of members of the three generations of Pgp-inhibitors (Fig. 1A), the inhibitors MRP1 (MK571, LY171883, BAY u9773, Fig. 1B) tend to have an amphiphilic structure with the clear hydrophilic moiety at the end opposite to the aromatic/hydrophobic one, while BCRP inhibitors (Ko143, FTC, Fig. 1C) seem to prefer 4- or 5-fused ring structures. Thus, the ligand-based design is still a predominant approach in the rational design of cancer EPIs, in particular in the case of ABCB1, thanks to the rich library of modulators identified so far.

In the last decade, our research team described numerous compounds targeting ABCB1 inhibitors in cancer cell lines belonging to the types of inhibitors shown in Fig. 1A [12-16]. In more detail, we were able to show highly potent ABCB1-inhibitory properties for aryl-piperazine hydantoin compounds [12, 14, 15]. The 5-aromatic substituted hydantoins were particularly potent [12, 15], while the potency decreased when the aromatic moiety was moved into position 3 [13]. Among the most active hydantoin-compounds found so far, the 5,5-diphenylhydantoin derivative **1** and spiro-fluorene derivative **2** (Fig. 2) were 4-7-fold more potent than the reference P-gp inhibitor verapamil, but they did not display either cytotoxic or antiproliferative activity towards cancer cell lines, *i.e.,* T-lymphoma [15] and NCI60 cell line panel (https://dtp.cancer.gov/discovery_development/nci-60/, data not published). In contrast, recent evidence indicates an increasing role of the triazine scaffold in potent hybrid anticancer agents [16], including 1,3,5-triazine-2,4-diamines [17, 18], especially, piperazine and morpholine derivatives displayed strong cytotoxic effects *in vitro* against NCI60 cancer cell lines [18].

Furthermore, our recent follow-up study was focused on aromatic selenoesters and seleno-anhydrides, possessing both anticancer and P-gp inhibitory properties [10]. The most active compounds **3** and **4** (Fig. 2), were tested in MDR mouse T-lymphoma cells overexpressing P-gp, displaying at the same time up to 3.4-fold more potent P-gp modulatory effect compared to the reference verapamil [19]. The main drawback of those selenoesters and seleno-anhydride lies in their low chemical stability and their very unpleasant intensive smell, limiting their further evaluation and potential therapeutic application.
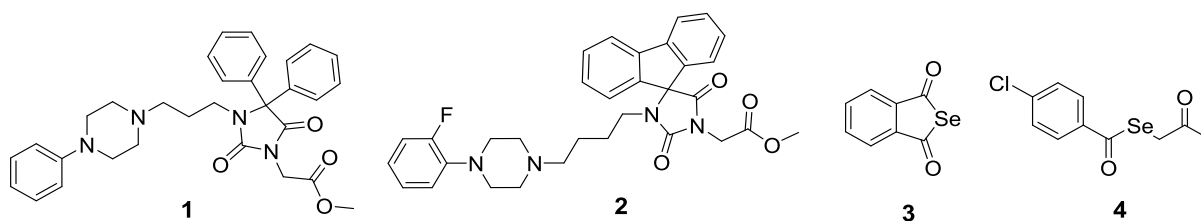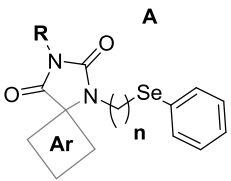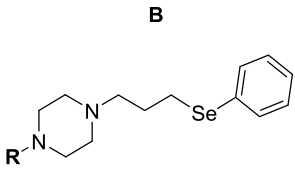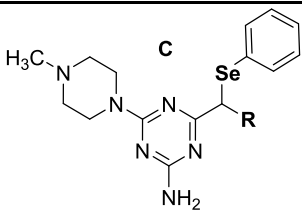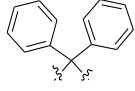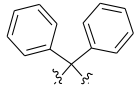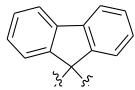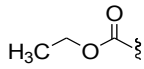
**Fig. 2** Hydantoin Pgp-modulators**, 1** and **2,** and seleno-compounds (**3** and **4**) with both anticancer and Pgp-modulatory properties found previously.

Taking into consideration the conclusions of previous studies [10, 12-19], and the fact that selenium in the form of ethers is chemically much more stable and devoid of any unpleasant smell, we decided to design and investigate a series of new phenylselenoethers with different aromatic/heterocyclic termination. In this study, a new series of compounds was designed as hybrid structures of both selenoethers and moieties found in the previous active P-gp inhibitors. We designed phenylselenoether derivatives, which can be divided into three main groups: (i) aryl-hydantoins and their bioisosteres with variable alkyl chain lengths (**5-7**, group A), (ii) (aryl)piperazines with various substituents at N-piperazine, including aromatic, alkyl and ester moieties (**8-13**, group B), as well as (iii) the 1,3,5-triazine scaffold with small C1-linker branches (**5-17**, group C, Table 2). The new hybrid compounds were synthesized and tested against P-gp in mouse T-lymphoma cells, then, their possible ability to regulate the cell proliferation rate and their cytotoxic effects were evaluated, as well. The best compounds **5-7** were further studied regarding the mechanism of ABCB1 modulation. For the most active compound (**6**), we extended our studies from the mouse cells to a cellular model of human T-lymphocytic cancer (JURKAT) [20], in order to evaluate its effects alone or in combination with the reference chemotherapeutic agent doxorubicin, as well as potential molecular mechanisms of action for the selenoether at a cellular level. Selected compounds, active in lymphocytic cancer cells, were also examined on their antiproliferative action in neuroblastoma cancer cell lines. Furthermore, we evaluated their drug-like properties, including lipophilicity, possible metabolic pathways, and potential drug-drug interactions (DDI) risks. Finally, qualitative structure-activity relationships (SAR) were discussed.

Thus, the goal of this work was a comprehensive study regarding differently substituted seleno-ethers (**5-17**, **Table 1**), in order to find new lead structure(s) in search of innovative anticancer drugs to overcome cancer MDR mechanisms.
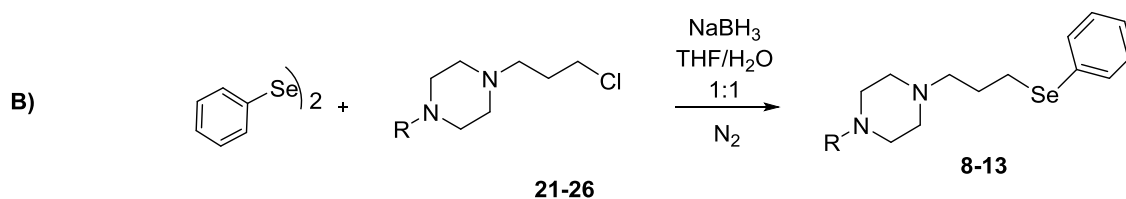
**Table 1** Chemical structures of compounds **5-17**



| Cpd | Gr. | Ar | R | n |
|-----|-----|-----|-----|-----|
| 5 | A | (diphenylmethyl) | -CH₂COOCH₃ | 4 |
| 6 | A | (diphenylmethyl) | -CH₂COOCH₃ | 6 |
| 7 | A | (fluorenyl) | -CH₃ | 4 |
| 8 | B | - | Ph | - |
| 9 | B | - | 2-MeO-Ph | - |
| 10 | B | - | 4-F-Ph | - |
| 11 | B | - | 3,4-diCl-Ph | - |
| 12 | B | - | -CH₃ | - |
| 13 | B | - | H₃C-CH₂-O-C(=O)- | - |
| 14 | C | - | -H | - |
| 15 | C | - | -CH₃ | - |
| 16 | C | - | C₂H₅ | - |
| 17 | C | - | diCH₃ | - |

# 2. Results and discussion

## 2.1. Chemical synthesis

Compounds **5-17** (Table 1) were obtained according to the synthesis route shown in Scheme 1. The hydantoin derivatives **5-7** (group A) were prepared applying a one-pot synthesis method, including Se-alkylation of previously described hydantoin intermediates **18-20** [14, 21-23]. In more detail, a reduction of the diphenyl diselenide to produce sodium selenolate was performed using sodium borohydride in water/tetrahydrofuran mixture (THF) 1/1 under a nitrogen atmosphere [23]. Upon decolourization of the solution, a suitably substituted hydantoin in dichloromethane (DCM) was injected without any need of a deprotonation salt to

produce the corresponding phenyl selenium hydantoins **5-7** in moderate yields and with excellent purity, within 3-4 days. (Scheme 1A).



**A)**

**18, 5:** Ar = R=-CH$_2$COOCH$_3$, n=4

**19,6** Ar = R=-CH$_2$COOCH$_3$, n=6

**20,7:** Ar = R=CH$_3$, n=4

**B)**
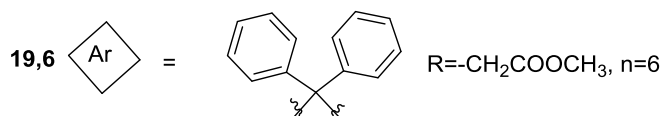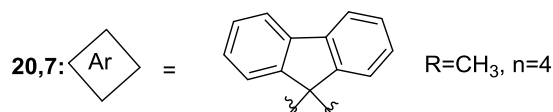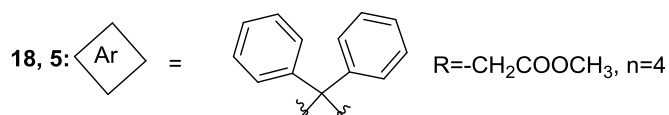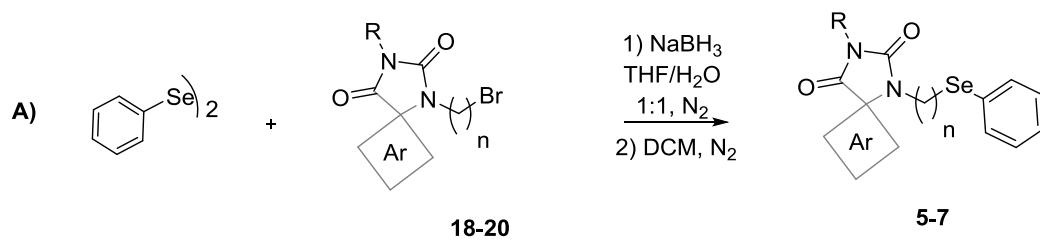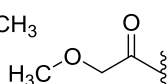
**21,8**: R= Ph
**22,9**: R=2-MeO-Ph

**23,10**: R= 4-F-Ph
**24,11**: R=3,4-diCl-Ph

**25,12**: R=-CH$_3$
**26,13**: R= H$_3$C-O-CH$_2$-C(O)-

**C)**
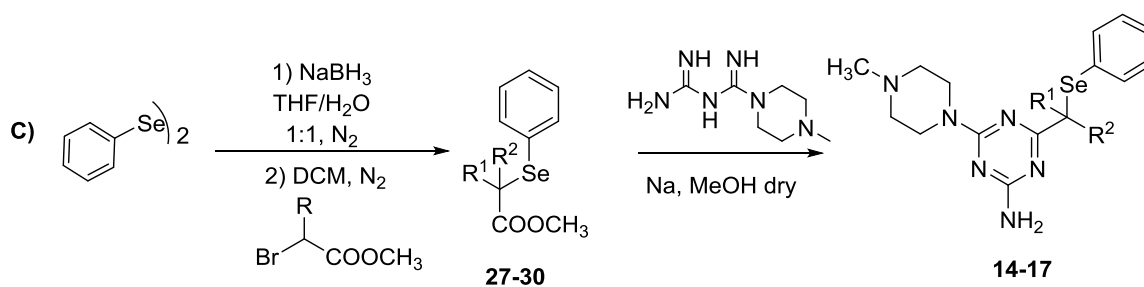
**27,14**: R1=R$^2$=H
**28,15**: R$^1$=CH$_3$, R$^2$=H

**29,16**: R$^1$=R$^2$= CH$_3$
**30,17**: R$^1$=C$_2$H$_5$, R$^2$=H

**Scheme 1.** Synthesis pathways of the final compound **5-17** and the relative intermediates **18-30.**

In the case of the phenyl selenium piperazine derivatives (**8-13**), the appropriate commercially available piperazines were alkylated using 1-bromo-3-chloropropane in the presence of anhydrous potassium carbonate in acetone as solvent at room temperature [24]. The so obtained crude intermediates were used applying the Se-alkylation method described for **5-7** (Scheme 1B).

1,3,5-Triazine selenium derivatives (**14-17**) were obtained as follows: firstly, the preparation of the sodium selenoate was carried out in a similar way as described for group A. The subsequent Se-alkylation was performed within 3-4 hours, without any need to use higher temperatures or deprotonation salt. The next step involved cyclic condensations in basic conditions with methyl piperazine biguanide, as previously described [23, 24].

Spectral and chromatographic analytical methods confirmed the structures and purity of the final compounds **5-17**. The intermediates (**21-30**) were either bought (**22** and **24)** or synthesized in the case of compounds **21, 23,** and **25-30** according to the previous methods [24-29]. The compounds **9-17** have been transformed into the corresponding crystalline hydrochloric salts for the relative biological studies.

## 2.2. Pharmacology

### 2.2.1. Efflux modulating effects

Compounds **5-17** (Table 1) were evaluated for their efflux modulating effects in mouse T-lymphoma cell line transfected with the human *MDR1* gene that codes for the ABC transporter ABCB1 measuring the accumulation of rhodamine 123, which is a substrate for ABCB1 [12, 30-32]. The percentage of mean fluorescence intensity was calculated for the treated MDR cells compared to the untreated cells, and then a fluorescence activity ratio (FAR) was determined. Verapamil was tested at the commonly used concentration (20 μM). All compounds (**5-17**) were investigated at the 10-fold lower concentration (2 μM) while weakly-active ones (**8-10**, **12-17**) also at the concentration of verapamil. In the case of the active modulators at 2 μM (FAR>2, **5-7**, **11**), the FAR values were determined at a low concentration of 0.2 μM, as well. Results are presented in Table 2.

**Table 2** Effects of compounds **5-17** on rhodamine 123 retention by human *MDR1 (ABCB1)* gene-transfected mouse lymphoma cells

| Compounds | FAR (0.2 µM) | FAR (2 µM) | FAR (20 µM) |
|---|---|---|---|
| DMSO (2 v/v%) | FAR (Control) 0.84 | | |
| Verapamil | - | - | 17.59 |
| **5** | 2.47 | 42.91 | - |
| **6** | 2.77 | 24.20 | - |
| **7** | 1.09 | 45.05 | - |
| **8** | - | 1.07 | 1.57 |
| **9** | - | 0.92 | 1.02 |
| **10** | - | 1.07 | 4.25 |
| **11** | 1.07 | 2.27 | - |
| **12** | - | 0.97 | 0.85 |
| **13** | - | 0.75 | 0.96 |
| **14** | - | 0.82 | 0.87 |
| **15** | - | 0.83 | 0.95 |
| **16** | - | 0.93 | 1.13 |
| **17** | - | 1.11 | 1.40 |

FAR, Fluorescence activity ratio was calculated using the following equation:

$$FAR = \frac{MDR_{treated}/MDR_{control}}{parental_{treated}/parental_{control}}$$

The inhibition of ABCB1 transporter is evident when FAR >1. [32] Since the treatment had no effect on the parental cells (PAR) lacking the overexpressed ABCB1 system, the intensity of fluorescence did not change in the treated cells compared to the control ones, for this reason, the denominator was considered as 1.

Among the evaluated derivatives, the compounds **5-7** (tested at 2 µM) displayed strong inhibitory potency, being up to 2.6-fold more effective than the reference inhibitor verapamil (at 20 µM). Other compounds (**10**, **11**), had significantly lower inhibitory activities (FAR 2.27 at 2 µM or 4.25 at 20 µM), while compounds **8**, **9** and **12-17** were inactive (Table 2).

*2.2.1.1. Studies on ABCB1 modulating mechanisms of compounds 5-7*

The most active compounds found in the rhodamine 123 accumulation assay (**5-7**) were tested at 100 µM on their influence on ATPase activity of Pgp pump in the luminescence Pgp-Glo™ Assay, according to previously described methods and protocols [33-35] (Fig. 3). In this assay, the Pgp-dependent decreases in luminescence are measured to reflect its increased ATP consumption. The ABCB1 basal ATP consumption (basal activity) is considered as a difference between the luminescent signal of samples treated with sodium orthovanadate, the selective and potent Pgp inhibitor (100% inhibition observed), and the luminescence of untreated Pgp samples. Thus, inhibitors give lower values (<100% of the basal activity), while the pump stimulators/substrates cause a statistically significant increase of the basal activity.

Verapamil at 200 µM was used as a reference modulator with the substrate/ATPase stimulatory mode of action, and caffeine as a reference inactive towards ABCB1 transporter to give negative control.

The obtained results showed that all compounds **5-7** significantly increased ($p<0.001$, $p<0.0001$) the Pgp basal activity in a similar way, but stronger, than verapamil (Fig. 3). These results are in line with those from the rhodamine 123 efflux assay, where stronger effects for **5-7** in respect verapamil were also found.
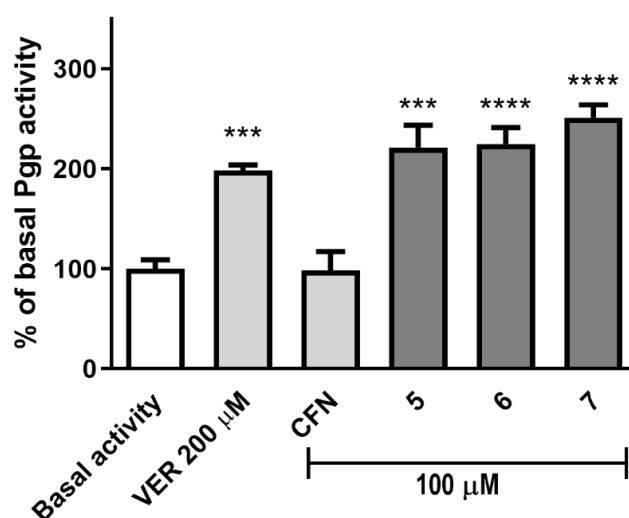


**Fig. 3** The effect of the ABCB1 substrate verapamil (VER) (200 µM), ABCB1-negative compound caffeine (CFN) (100 µM) and compounds **5, 6** and **7** (100 µM) on ABCB1 basal activity. The compounds are recognized as an ABCB1 substrate if they stimulate their basal activity (>100%). Data are presented as the mean ± SD. Statistical significance was evaluated by one-way ANOVA, followed by Bonferroni's comparison test (***$p<0.001$, ****$p<0.0001$ compared with the basal activity).

Summing up, compounds **5-7** did not inhibit the work of Pgp pump in this assay but displayed a substrate property. Thus, the putative mechanism of the dye-substrate efflux inhibition caused by **5-7** (Table 2) was the most probably associated with a competitive displacement in the substrate-binding site of this MDR transporter.

### 2.2.2. Cytotoxic and anti-proliferative effects

The whole series (**5-17**) was also examined on their cytotoxic and anti-proliferative activity in both sensitive (PAR) and resistant (MDR) mouse T-lymphoma cell lines (Table 3).

**Table 3** Cytotoxic and antiproliferative effect of the compounds **5-17** on sensitive parental (PAR) and resistant (MDR) mouse T-lymphoma cells

| Compound | Cytotoxic effects | | Antiproliferative effects | |
|---|---|---|---|---|
| | PAR mean $IC_{50}$ ($\mu$M) $\pm$ SD | MDR mean $IC_{50}$ ($\mu$M) $\pm$ SD | PAR mean $IC_{50}$ ($\mu$M) $\pm$ SD | MDR mean $IC_{50}$ ($\mu$M) $\pm$ SD |
| **5** | $2.91 \pm 0.18$ | $3.39 \pm 0.09$ | $16.75 \pm 1.37$ | $7.82 \pm 0.57$ |
| **6** | $0.67 \pm 0.03$ | $0.90 \pm 0.07$ | $3.84 \pm 0.05$ | $1.34 \pm 0.05$ |
| **7** | $3.25 \pm 0.11$ | $4.21 \pm 0.40$ | $12.53 \pm 0.95$ | $4.67 \pm 0.38$ |
| **8** | $21.50 \pm 0.24$ | $44.35 \pm 2.88$ | $28.96 \pm 2.30$ | $13.07 \pm 0.97$ |
| **9** | >100 | >100 | >100 | $71.94 \pm 4.30$ |
| **10** | $6.55 \pm 0.53$ | $29.09 \pm 0.97$ | $13.92 \pm 0.07$ | $7.67 \pm 0.84$ |
| **11** | $2.27 \pm 0.26$ | $3.50 \pm 0.29$ | $17.04 \pm 2.22$ | $3.66 \pm 1.23$ |
| **12** | $60.59 \pm 0.98$ | $98.56 \pm 0.64$ | $62.91 \pm 3.03$ | $23.40 \pm 1.22$ |
| **13** | $51.56 \pm 1.30$ | $75.70 \pm 3.31$ | $53.72 \pm 1.71$ | $37.67 \pm 1.95$ |
| **14** | >100 | >100 | >100 | >100 |
| **15** | >100 | >100 | $38.12 \pm 1.74$ | $28.93 \pm 1.89$ |
| **16** | $84.93 \pm 1.36$ | >100 | $65.16 \pm 1.36$ | $48.47 \pm 2.56$ |
| **17** | >100 | >100 | $35.29 \pm 1.07$ | $8.28 \pm 1.47$ |

The tested compounds **5-7** and **11** showed very high cytotoxic effects in both MDR and PAR cell lines ($IC_{50}$< 5 $\mu$M), with compound **6** presenting the highest activity among the tested selenoethers. Most compounds of the series displayed lower cytotoxic concentrations for PAR T-lymphoma cells in comparison to MDR ones. This difference is particularly evident in the case of compound **10** (>4-fold) and **8** (>2-fold), and only slight in the case of the most cytotoxic compounds (**5-7** and **11**). Compounds **12, 13** with low cytotoxic effects in PAR cell lines were less potent in MDR cells too, while compounds **9** and **14-17** displayed no cytotoxicity in both PAR and MDR cell lines, even at a concentration of 100 $\mu$M (84 $\mu$M for **16** tested in PAR).

The series demonstrated unexpectedly interesting antiproliferative properties in MDR mouse T-lymphoma cells, as each member caused more potent antiproliferative effects in MDR than in PAR cells. Almost the whole series displayed $IC_{50}$ (MDR) lower than 100 $\mu$M, while **5-7, 10, 11,** and **17** lower than 10 $\mu$M. Similar to the cytotoxicity test results, compound **6** also displayed the most potent antiproliferative action for both PAR ($IC_{50}$= 3.83 $\mu$M) and MDR ($IC_{50}$ = 1.33 $\mu$M) cells, being the only member with $IC_{50}$<10$\mu$M in PAR cells. To sum up,

most of the compounds showed moderate antiproliferative properties in PAR cells, with $IC_{50}$ in the range of 12-65 μM, excluding **9** and **14**, which were inactive up to a concentration of 100 μM.

*2.2.3. Anticancer properties in JURKAT human T-lymphoblastic leukaemia cell line.*

*2.2.3.1. Effects of compound **6** on proliferation rate in JURKAT cells.*

Compound **6** was the best compound of our series so far in terms of antiproliferative and cytotoxic activities, as well endowed with significant efflux pump inhibitory properties in mouse T-lymphoma. In order to extend the analysis to a human cell context, representing an immortalized T lymphocyte cell line used as a model for acute lymphoblastic leukaemia (ALL) [36], we decided to explore the effect of compound **6** on proliferating JURKAT leukaemia cells. This cellular system represents a useful model for testing the effects of different compounds on cell metabolism [37] and proliferation rate [38]. The effects of compound **6** on either proliferation rate or cell cycle-related gene expression were examined alone or in combination with doxorubicin (a chemotherapeutic agent able to block tumour growth *in vivo*) in order to find whether the co-treatment should enhance the effect of doxorubicin [38-40]**.** Doxorubicin is a well-known and successful antineoplastic drug commonly used as a chemotherapeutic agent in various cancers, including ALL, but, at present, drug resistance is common [41, 42].

For these reasons, we performed proliferation assays in JURKAT cells treated with compound **6** at 0.1- 0.5 and 2 μM concentrations, alone or in combination with doxorubicin, tested at 50 and 250 nM at two distinct time points (24 and 72 hours).

While at early time compound **6** did not significantly affect cell proliferation rate, doxorubicin alone was able to block proliferation, especially at higher concentrations (Fig. 4A). Notably, at 72 hours post-treatment, a significant reduction in proliferation was observed in cells treated with compound **6** alone and with doxorubicin alone, but a more significant effect was detected in cells co-treated with both compound **6** and doxorubicin. These data highlighted a synergistic effect of compound **6** with doxorubicin, especially when compound **6** was added to cell cultures at a higher dose (2 μM) (Fig. 4B). In summary, these results indicate that the co-treatments with compound **6** and doxorubicin counteracted cell proliferation in JURKAT cells and that the co-treatment with compound **6** enhances the effect of doxorubicin.
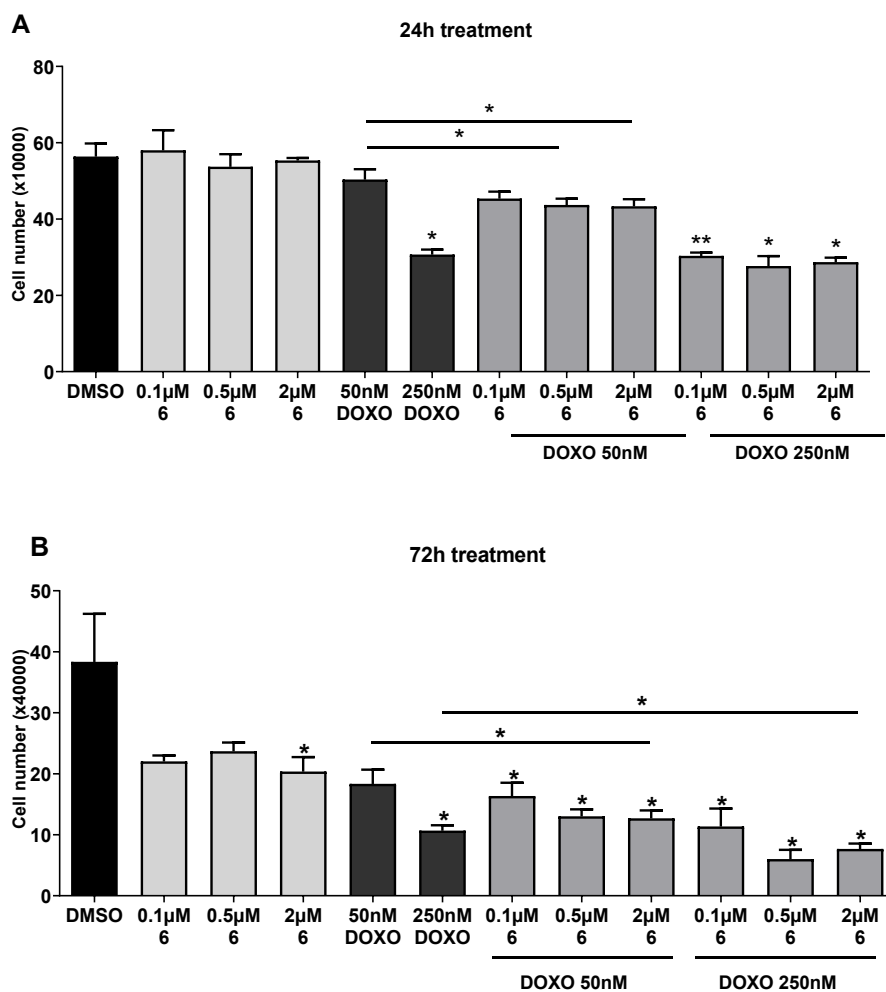
**Fig. 4.** Dose-response curves for anti-proliferation activity of compound **6** and doxorubicin in a dose range (0.1, 0.5, and 2 μM for compound **6** and 50 and 250 nM for doxorubicin) on JURKAT cells after 24 h (A) and 72 h (B) of treatment. The results represent the average cell number ± SEM of three independent experiments. Significance is represented as *$p < 0.05$ and **$p < 0.01$ related to control groups.

*2.2.3.2. Effects of compound 6 on cell cycle-related gene expression in JURKAT*

In order to estimate a potential molecular mechanism for the anticancer activity found for **6**, we focused on the expression levels of cyclin D1, a well-known gene related to cell cycle progression contributing to uncontrolled proliferation and found to be negatively regulated in a previous study by the treatment with a selenium-containing compound in gastric cancer [20]. In addition, we analysed the expression level of p53 involved in apoptotic response, cell cycle arrest, and senescence [43].

In order to understand whether compound **6** was able to limit cell proliferation through gene expression regulation of cyclin D1 and p53, we treated JURKAT cells with compound **6** at

15

three concentrations (0.1, 0.5 and 2 μM) and doxorubicin (50 nM), analysing with RT-PCR the mRNA transcripts levels of cyclin D1 and p53. DMSO was used as a negative control.

The results depicted in Fig. 5 show that compound **6** was able to significantly reduce cyclin D1 expression and increase the level of p53 (Fig. 5A), already after 24 hours of treatment. Moreover, the co-treatment with both compound **6** and doxorubicin enhanced the effect of the single treatments on gene expression.
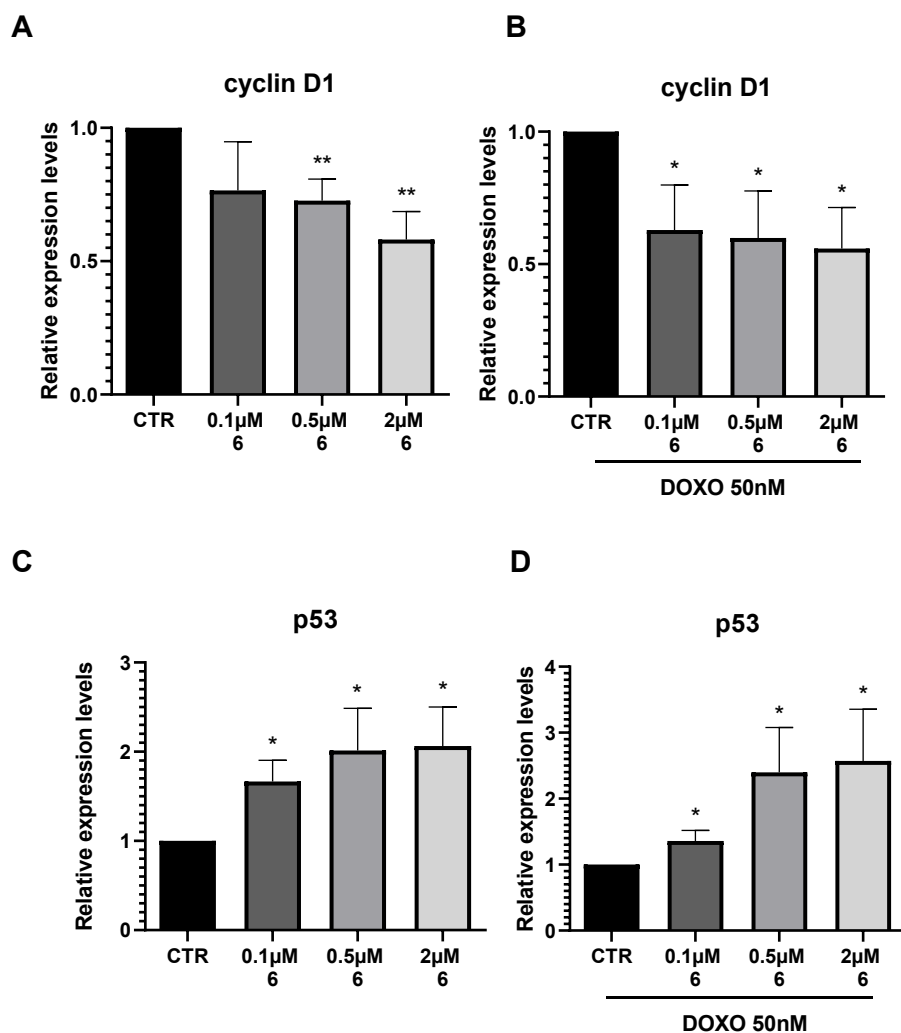


**Fig. 5.** (A-C) JURKAT cells were treated with compound **6** (0,1 - 0,5 or 2 μM) alone or (B-D) in combination with doxorubicin (50nM) or with DMSO (CTR), as a control, for 24 hours. Expression of cyclinD1 (A-B) and p53 (C-D) mRNAs were evaluated on total RNA by qRT-PCR. Bars represent means ± SEM of 6 experiments.

To sum up, these results indicate that compound **6** inhibited cell cycle progression through the reduction of the expression of cyclin D1 and inhibited cell proliferation by inducing p53 expression.

*2.2.4. Anticancer action against neuroblastoma cancer cells*

In order to estimate a broader range of anti-cancer potency, including also non-lymphocytic cancer cells, an influence of the most active selenoethers **5-7** on neuroblastoma cancer proliferation was investigated in SH-SY5Y cells affecting their viability (Fig. 6). The results show that all tested compounds at a concentration of 10 μM significantly inhibited cell proliferation up to 60%. Compounds **6** and **7** were the most active ones, inhibiting cell growth by 12% and 8%, respectively, already at a concentration of 0.5 μM, while the compound **5** was active only at 10 μM.
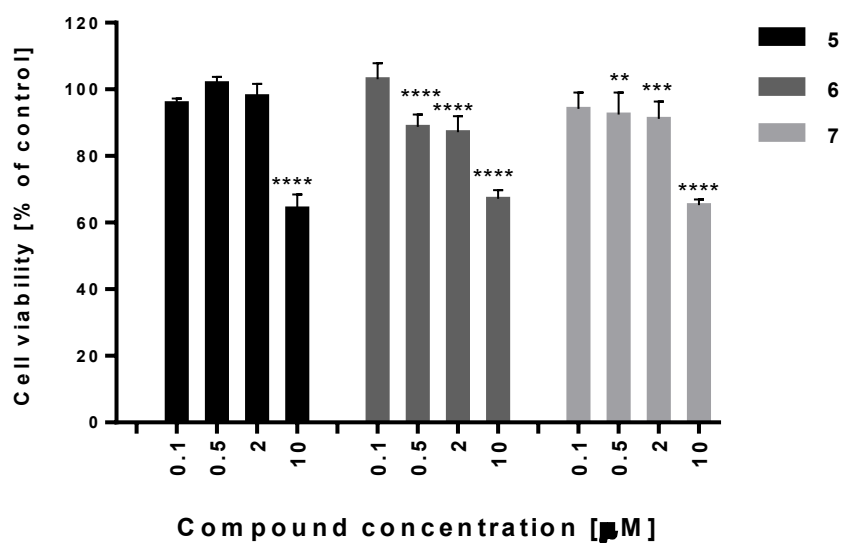


**Fig. 6.** Effect of selenoethers **5-7** on neuroblastoma cell viability. SH-SY5Y cells were incubated for 72 h in the presence of the compounds **5-7** at a concentration of 0.1, 0.5, 2, 10 [μM]. Cell viability was measured by MTS assay. Each point (mean ± SEM of two independent experiments, each of which consisted of six replicates per treatment group) represents absorbance units and is expressed as a percentage of control compared to 0.1% DMSO control cells (set as 100%). Statistical analysis by one-way ANOVA showed significant differences between the groups ($P<0.05$) and was followed by the Bonferroni multiple comparison test. Data indicated with ****$P \leq 0.0001$, ***$P \leq 0.001$, **$P \leq 0.01$ reflects statistically significant differences between control and experimental groups.

## 2.4. Drug-likeness in vitro
### 2.4.1. Lipophilicity

In the presented work, the lipophilicity of the selenoethers was estimated using standard RP-TLC method. Retention parameters for the compounds were designated and analysed to give

$R_{M0}$ values that reflect the lipophilic properties of the tested compounds (details in Table S1, Supplementary).

The $R_{M0}$ values of the tested compounds ranged from 0.79 to 6.05 (Fig. 7) and were corresponding to structural differences of the compounds. Thus, group A of hydantoin derivatives (**5-7**) was more lipophilic than both, group B of phenylpiperazine selenoethers (**9-13**) and C of 1,3,5-triazine derivatives (**14-17**). In the case of group B, the significant internal diversity of lipophilic properties between aromatic- (**9-11**) and non-aromatic piperazine (**12, 13**) compounds was seen in good accordance with the piperazine substituent properties. In contrast, most of the members of group C (**14, 15** and **17**) demonstrated almost identical lipophilic character. Taking into consideration the results, lipophilic-dependent trends can be observed for the ABCB1 modulatory action examined (Table 2). Thus the most lipophilic hydantoin derivatives (**6-7**) displayed significantly stronger action than either piperazine (**9-13**) or triazine (**14-17**) ones. Furthermore, compound **6,** the outstanding one in terms of cytotoxicity and antiproliferative properties in the cancer cells, was also the most lipophilic within the series.
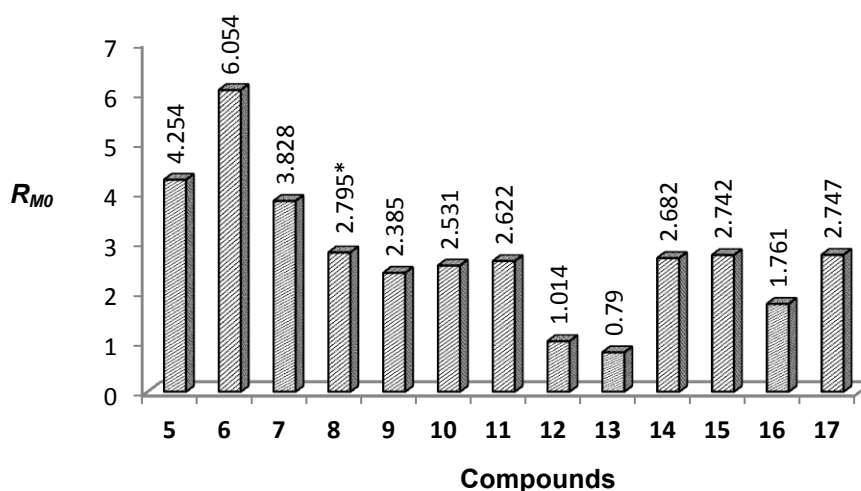


**Fig. 7.** Lipophilicity data for compounds **5-17**. * Lipophilicity tested for the basic form (**8**), unlike the hydrochloric salts of the rest of group B (**9-17**). This relatively overstated lipophilicity of **8**, as not comparable, was excluded from the discussion on results.

### 2.4.2. Metabolic stability in vitro

The metabolic stability of selenoorganic compounds **5-7** was investigated using mouse liver microsomes (MLMs). The UPLC spectra of the reaction mixtures after 120 min incubation with MLMs showed that all examined compounds were metabolically unstable

(Fig. 8).
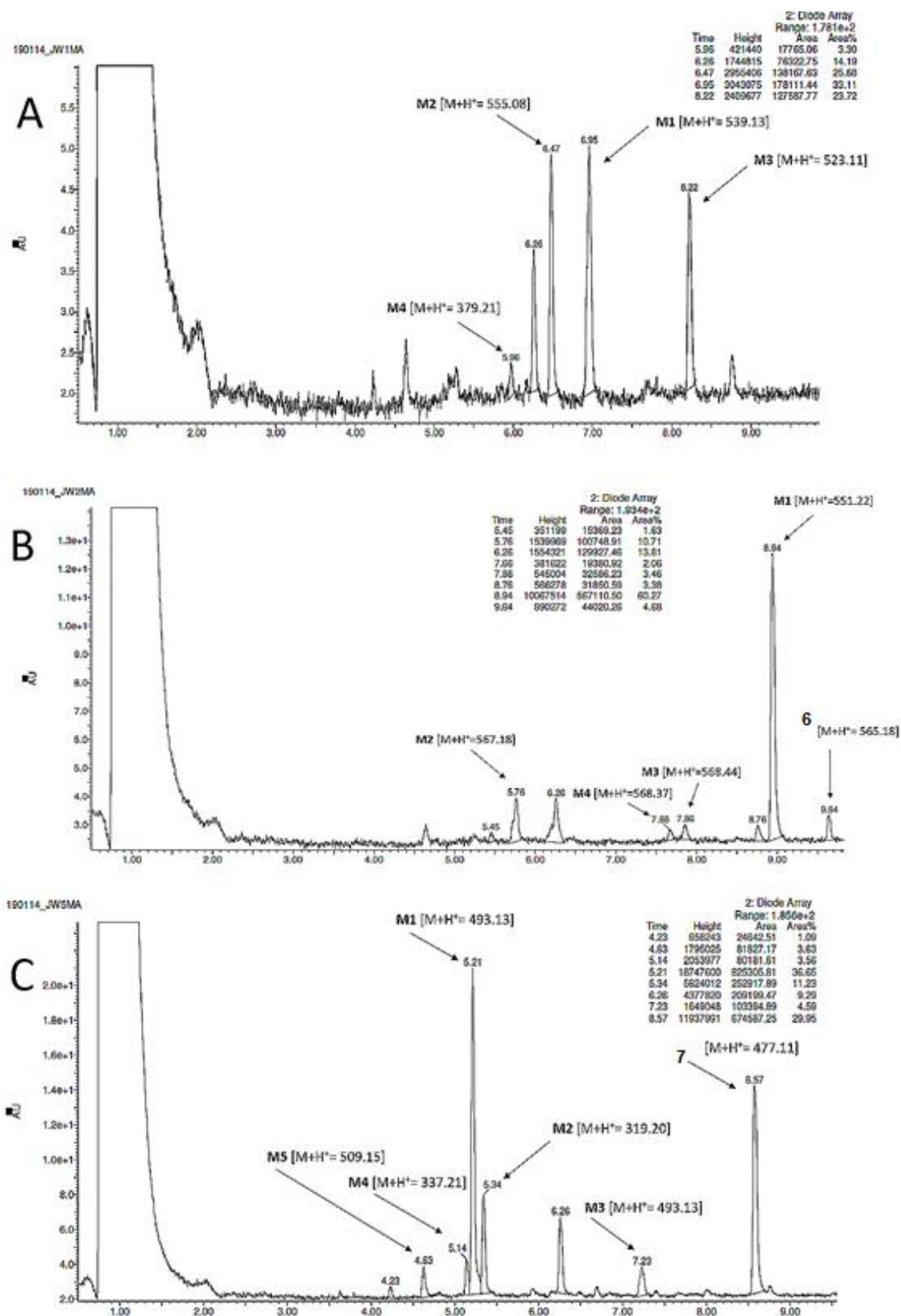


**Fig. 8.** UPLC spectra of the reaction mixtures after 120 min incubation of selenoethers **5** (A), **6**(B) and **7** (C) with MLMs. The peak at the retention time 6.26 min was identified as the contamination.

Compound **5** was metabolized completely into four metabolites M1-M4, as no parent compound was observed at UPLC spectra (Fig. 8A). Only a slight amount (4.5%) of compound **6** remained in the reaction mixture. This compound was biotransformed mainly into metabolite M1 and small amounts of three more metabolites M2-M4 (Fig. 8B). Compound **7** was metabolized mainly into metabolite M1 and four more metabolites M2-M5 (Fig. 8C).

According to UPLC spectra, compound **7** was determined as the most stable among the tested series, as around 30% of this compound remained in the reaction mixture. The performed next MS and precise ion fragment analyses of the parent compounds and their metabolites allowed for a determination of the metabolic pathways and the most probable structures of metabolites among tested series. Generally, the most common metabolic pathways of **5** and **6** were ester hydrolysis and hydroxylation (Fig. S1A-C and S2A-D, Supplementary information). Compound **7** was mostly hydroxylated and decomposed at Se atom (Fig. S3A-E, Supplementary information). A similar to **7** decomposition pattern for Se was also observed for compound **5** (Fig. S1D and S3B, Supplementary information). All metabolic pathways of the tested selenoethers were summarized in Table 4.

**Table 4** The molecular masses and metabolic pathways of compounds **5-7**.

| Substrate | Molecular mass ($m/z$) | Number of identified metabolites | Molecular mass of the metabolite ($m/z$) | Metabolic pathway |
|---|---|---|---|---|
| **5** | 537.14 | 4 | 539.13 (**M1**) | *ester bond hydrolysis, hydroxylation* |
|  |  |  | 555.08 (**M2**) | *ester bond hydrolysis, double hydroxylation* |
|  |  |  | 523.11 (**M3**) | *ester bond hydrolysis* |
|  |  |  | 379.21 (**M4**) | *decomposition at the Se atom* |
| **6** | 565.18 | 4 | 551.22 (**M1**) | *ester bond hydrolysis,* |
|  |  |  | 567.18 (**M2**) | *ester bond hydrolysis, hydroxylation* |
|  |  |  | 568.44 (**M3**) | *ester bond hydrolysis, ketone reduction, hydroxylation* |
|  |  |  | 568.37 (**M4**) | *ester bond hydrolysis, ketone reduction, hydroxylation* |
| **7** | 477.11 | 5 | 493.13 (**M1**) | *hydroxylation* |
|  |  |  | 319.20 (**M2**) | *decomposition at the Se atom* |
|  |  |  | 493.13 (**M3**) | *hydroxylation* |
|  |  |  | 337.21 (**M4**) | *decomposition at the Se atom, hydroxylation* |
|  |  |  | 509.15 (**M5**) | *double hydroxylation* |

*2.4.3. Drug-drug interactions prediction*

The potential drug-drug interactions (DDI) of selenoethers **5-7** were predicted by *in vitro* assessment of their effect on CYP3A4 isoform being the most involved in drug metabolism. The compounds **5-7** were screened at 10 μM, and the results were compared to the reference selective CYP3A4 inhibitor ketoconazole. All examined compounds in a statistically significant manner (****$p < 0.0001$) reduced CYP3A4 activity (Fig. 9).
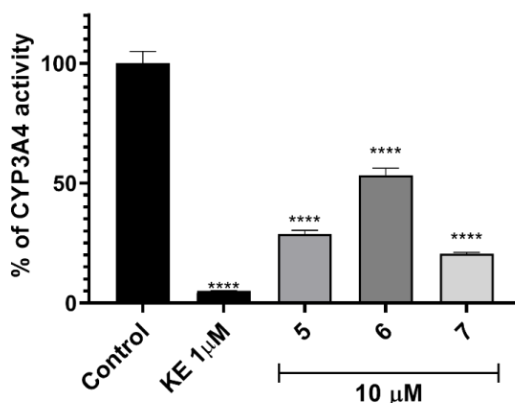


**Fig. 9.** The influence of selenoethers **5-7,** and the reference inhibitor ketoconazole (KE) on CYP3A4 activity. The statistical significance was evaluated by a one-way ANOVA, followed by Bonferroni's Multiple Comparison Test (****$p < 0.0001$ compared with untreated control).

The weakest inhibition was shown for compound **6**, which reduced CYP3A4 activity up to ~53% of untreated control, whereas **5** and **7** decreased its activity up to 28 and 20%, respectively. However, the observed effects of **5-7** were much weaker than that for the reference drug ketoconazole, which reduced almost entirely CYP3A4 activity at 1 μM (Fig. 9).

*2.5. General and SAR discussion*

In order to find new anticancer hybrids able to overcome MDR mechanisms, we explored the chemical space of moieties that were useful to join the phenylselenoether fragment as a fixed scaffold, including selenoether linkers. Our rational design of suitable moieties based on results coming from recent literature evidence [16-18] or our previous experiences in searching anticancer and anti-MDR agents [10-15]. In this context, our present modifications divided the chemical space of the phenylselenoether derivatives into three main groups*, i.e.,* 5-arylhydantoin derived compounds (**5-7,** group A), aryl- (**8-11**), alkyl- (**12**) or ester- (**13**) piperazine derivatives (group B) and 1,3,5-triazine derivatives with different alkyl branches within the Se-ether linker (**14-17**, group C). The comprehensive biological screening,

including cancer efflux pump inhibitory-, cytotoxic and antiproliferative properties for whole the series (**5-17**) on the one hand, and ADMET *in vitro* studies for selected compounds **5-7**, on the other hand, has provided exciting and even unexpected qualitative structure-activity relationship (Fig. 10).
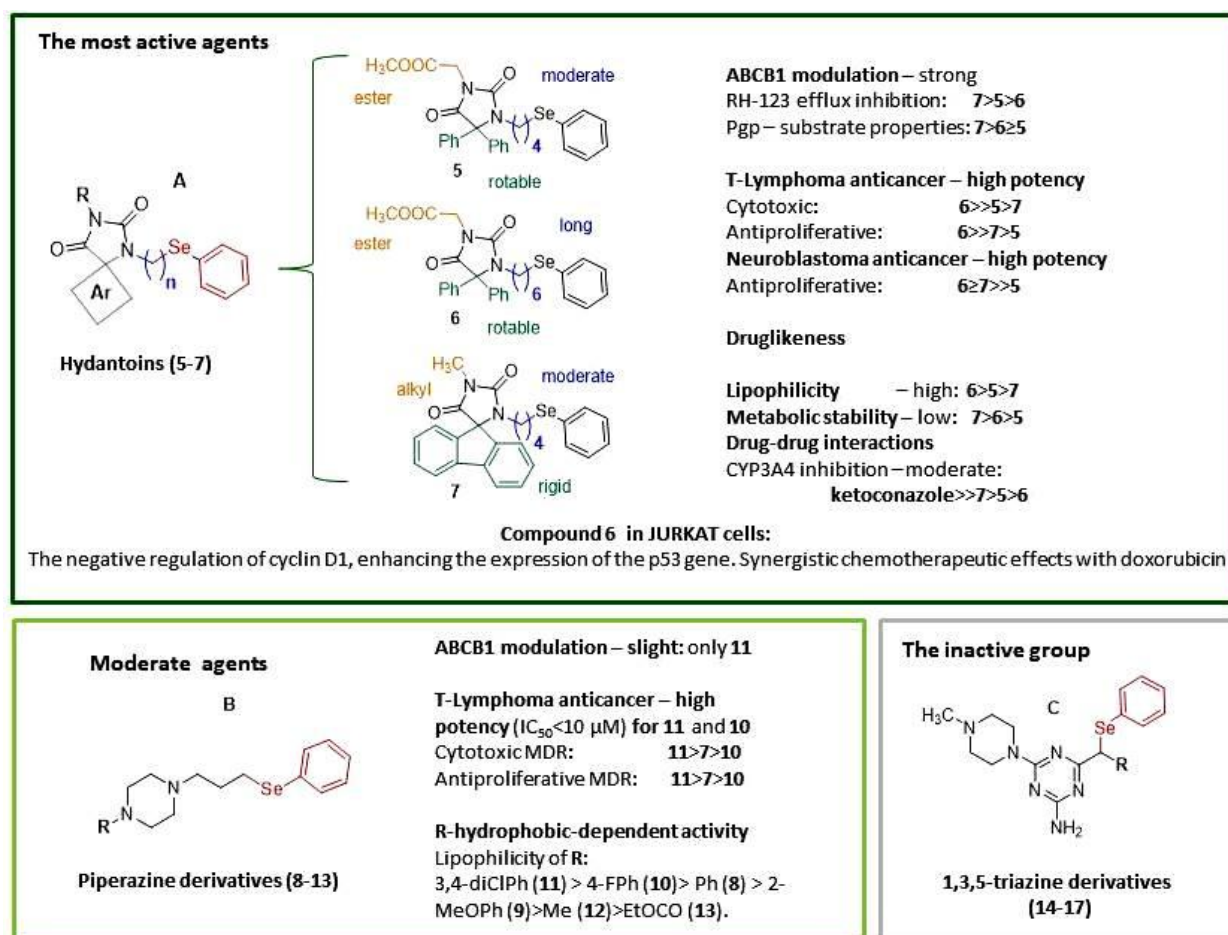


**Fig. 10.** SAR overview of compounds **5-17.** The common phenylselenoether (red) moiety is probably responsible for the trend of more potent antiproliferative activity in the resistant T-lymphoma (MDR), than that in sensitive (PAR) cells in all three series A-C. Advantage of these new-discovered hydantoin selenoethers (red), referring to previous Se-esters, is the lack of any unpleasant smell and their higher chemical stability

Among the three considered groups, hydantoin derivatives (group A, **5-7**) were found to be the most promising structural moiety, being up to 2.6-fold more effective MDR EPI (at a 10-fold lower concentration) than the reference ABCB1-inhibitor verapamil. These compunds possessed also significant ABCB1 substrate potency in Pgp ATPase test, significantly higher than that of reference verapamil. Both assays indicated the realtively strongest effect for the compound with the rigid spirofluorene moiety (**7**), if comparing to **5** and **6** containing rotable 5,5-diphenyl moiety (marked in green, Fig. 10).Furthermore, all three members (**5-7**)

displayed significant cytotoxic and antiproliferative properties in the MDR cancer cells of T-lymphoma. The length of the linker seems to be of considerable importance, as 5,5-diphenylhydantoin compound **6** (IC$_{50}$ <1.5 μM in both cases, Table 3) with the longest (C6) linker was the best one of the present study. Taking into account our previous results, both 5,5-diphenylhydantoin and 5-spirofluorenehydantoin moieties, appeared in the structures of highly potent arylpiperazine ABCB1-inhibitors [14]. Their combination with a phenylpiperazine moiety gave even stronger inhibitory effects than those observed in this study, more than 20-fold stronger than verapamil [32]. However, those compounds displayed neither cytotoxic nor antiproliferative actions on cancer cells (T-lymphoma).

Furthermore, a too potent ABCB1-inhibitory property can be considered as risky for host organisms, taking into consideration the role of ABC-transporters in healthy human cells, which protect them from toxic substances or drugs. From a therapeutic point of view, the identified pharmacological properties of seleno-diphenylhydantoin **6** seem to be much more promising, and thus provides a new therapeutic direction for structural derivatives of anticonvulsant drug phenytoin (5,5-diphenylhydantoin). It should be noted that the hydantoin scaffold is a common motive in other anticancer drugs, *e.g.,* the 5,5-dimethylhydantoin derivative, nilutamide. However, our previous studies on the series of 5,5-dimethylhydantoin derivatives indicated a weaker (usually negligible) ABCB1-inhibitory properties in T-lymphoma in comparison to their 5,5-diphenyl analogues [13, 14, 32].

Comparing the piperazine phenylselenoethers (**8-13**, group B) to hydantoins (**5-7**), the phenylpiperazine subgroup demonstrated generally lower pharmacological effects but with notable mutual differences, almost regular and highly corresponding to their structural traits. The structural difference of compounds **8-13** concerns substituents at N-piperazine, including aromatic, alkyl and ester moieties, which influence the hydrophobic properties of the subseries, in the following order: 3,4-diClPh (**11**) > 4-FPh (**10**)> Ph (**8**) > 2-MeOPh (**9**)>Me (**12**)>EtOCO (**13**). Almost an identical order can be observed for both ABCB1-inhibitory and anticancer properties, including cytotoxic and antiproliferative actions (Tables 2 and 3). The biggest and most hydrophobic 3,4-dichlorophenyl substituted compound (**11**) was outstanding in the field of the efflux pump modulatory action (FAR=2.27 at 2 μM), also exceeding the rest of group B in cytotoxic (IC$_{50}$=3.50 μM) and antiproliferative action (IC$_{50}$=3.66 μM). The 4-fluorophenyl derivative (**10**), the next in the hydrophobicity order, displayed some EPI properties at the high concentration (FAR=4.25 at 20 μM), but was especially potent in terms of antiproliferative action in the MDR T-lymphoma (IC$_{50}$=3.50 μM). It is worth to underline

that both, **11** and **10**, displayed corresponding or even slightly stronger antiproliferative properties than those of hydantoin derivatives **5** and **7**, respectively (Table 3).

The last subseries of the triazine phenylselenoethers (**14-17,** group C) was surprisingly inactive, taking into consideration increasing literature evidence indicating a beneficial role of the 1,3,5-triazine scaffold in various cancers [16-18]. This small subseries differs only in the field of the C1-linker branches, which undoubtedly influence slightly hydrophobicity and the steric hindrance/flexibility due to the variety of the spacer. In this group, only the dimethyl-branched derivative **17** displayed notable antiproliferative property in MDR T-lymphoma (IC$_{50}$ =8.28 μM). It should be noted that the antiproliferative action of compound **17** is almost 4-fold more potent in the MDR- than in the PAR cells.

The trends of more potent antiproliferative activity in the resistant T-lymphoma (MDR), than that in sensitive (PAR) cells, was noted for all three series A-C (Table 3). It suggests that the phenylselenoether moiety, as the characteristic common feature, is responsible for this favourable behaviour (marked in red, Fig. 10), while changeable moieties could modulate the intensity of this effect. The strongest result was observed for the 3,4-dichlorophenylpiperazine derivative **11** and the aforementioned triazine derivative **17**.

Comparing the lack of anticancer action in previous studies for the hydantoin-phenylpiperazines [14, 32] to the significant effects found in this study (groups A and B), it is not hard to recognize that the selenoether linker is the most probable structural factor, responsible for an introduction of both, the cytotoxic and antiproliferative, properties into the considered chemical families of hydantoin and phenylpiperazines. Likewise, the length of the linker seems to be crucial. It catches the eye that the most active hydantoin derivative **6**, distinctly predominant in the whole series is only one that contains the longest C6-linker, while the anticancer action is decreasing with C4-linker (**5** and **7**) and C3-linker of phenylpiperazine derivatives (**8-13,** group B), to be the weakest in the case of short and rather stiff C1-linkers of 1,3,5-triazine derivatives **14-17** (group C). This is especially noticeable in the results of cytotoxic properties in both MDR and PAR T-lymphoma cells (Table 3).

Analysing the present results for the new Se-ether compounds (**5-17**) in comparison to those for the previous selenoesters (**4**) and selenoanhydride (**3,** Fig. 1) [15], corresponding efflux pump inhibitory and cytotoxic effects in MDR T-lymphoma can be observed. In more detail, the ABCB1-inhibitory properties of the most active hydantoin-selenoethers (**5-7**) were in the range of 1.38-2.56 of the action of verapamil (at a 10-fold higher concentration), while

they were 1.57 and 3.43, tested in the same conditions for the selenoanhydride **3** and selenoester **4**, respectively. In the case of cytotoxic action in MDR T-lymphoma, the $IC_{50}$ values were 4.65 μM (**3**) and 1.03 μM (**4**) *vs* 0.90-4.21 μM for the best selenoethers found in this study. Interestingly the most active compounds (**5-7)** were also active in neuroblastoma SH-SY5Y cells.

On the other hand, an undeniable advantage of these new-discovered hydantoin selenoethers, referring to previous Se-esters, is the lack of any unpleasant smell and their higher chemical stability observed in the test conditions. Furthermore, the results of the assays using an *in vitro* CYP3A4 model for most active compounds (**5-7)** demonstrated their low DDI risk in comparison to ketoconazole (Fig. 9). However, their metabolic stability tested in mouse microsomes was rather low; the highest stability was observed in the case of the spirofluorene derivative (**7**). These results require further scientific considerations, *i.e.,* more comprehensive studies on biotransformation of **5-7** and their potential metabolites, also using human metabolism models, as well as an estimation of the intrinsic anticancer/ MDR EPI properties of the most probable metabolites. On the other hand, further rational pharmacomodulations to improve metabolic stability and general "drugability" within this interesting new group of hydantoin-selenoethers is needed.

This study also provided an insight into potential molecular mechanisms of actions for the hydantoin-selenoether compounds. In order to explore the biological effects of the best compound determined from the mouse T-lymphoma assays, the longest-linker hydantoin derivative **6**, was evaluated in JURKAT human lymphoblastoid cells since these cells represent a good system to study drug resistance, cell death and proliferation in response to drugs treatment [38]. It has been reported in colon cancer cells that selenium shows chemotherapeutic potential against cancer cells by inactivating AKT and leading to suppression of cyclin D1 while triggering apoptosis [39]. Notably, methylselenol exposure changed the expression of genes related to the regulation of cell cycle and apoptosis, among which the tumour suppressor gene p53 [40]. Thus, we focused on the regulation of proliferation rate and on cyclinD1 and p53 expression. We were pleased to observe that the selenium-containing compound **6** inhibited cell proliferation through the negative regulation of cyclin D1, while enhanced the expression of the p53 gene. Furthermore, the co-treatment of JURKAT cells with doxorubicin and our compound enhances the chemotherapeutic effect of this drug, suggesting a synergistic activity warranting further studies. This effect is evident and statistically significant especially after 72 hours of treatment and when compound **6** is

used at the higher dose tested (2 μM). At the present this data indicate the effectiveness of strategies based on different compound combinations to enhance the activity of commonly used antineoplastic drugs.

## 3. Conclusions

In the present work, we have discussed a new chemical family of potent selenium-containing compounds as hybrids of phenylselenoethers with either arylhydantoin or phenylpiperazine moieties. Comprehensive studies, *i.e.,* design, synthesis and both, biological and ADMET-screening *in vitro,* including an insight into cellular mechanisms of anticancer action and followed by in-depth SAR analysis, have been performed, yielding promising results.

Among the new hybrids (**5-17**), the hydantoin derivatives (**5**, **6,** and **7**) were significantly more effective than the reference inhibitor verapamil (up to 2.6-fold at a 10-fold lower concentration) in order to inhibit the crucial tumour MDR mechanism of ABCB1-efflux pump. The very high stimulation of Pgp efflux pump (>200% of Pgp basal activity) at the presence of **5-7** confirmed their substrate potency and the probable competitive action with 123 rhodamine to the binding site in ABCB1-efflux modulating assay. Next, the cytotoxic and anti-proliferative action in both, sensitive (PAR) and resistant (MDR), mouse T-lymphoma cell lines revealed that both hydantoin- (**5-7**) and phenylpiperazine-selenoethers (**10** and **11**) possessed a good activity profile, being the 5,5-diphenylhydantoin compound (**6**) the best one out of the complete series. The promising antiproliferative action of the hydantoin compounds **6** and **7** were confirmed additionally in non-lymphocytic cancer cells, *i.e.* neuroblastoma, suggesting a therapeutically-promising broader spectrum of anticancer potency for this chemical family, also with an accent on the longer-linker compound (**6**). The mechanistic study results indicate that compound **6** inhibits cell cycle progression through the reduction of the expression of cyclin D1 and cell proliferation by inducing p53 expression, thus giving a first insight into the mechanism of action. Furthermore, the SAR analysis proved that the lipophilic properties, together with a longer selenoether spacer, are the likely factors affecting all, cancer EPI-, antiproliferative- and cytotoxic effects, in the tested cancer models for the new family of selenocompounds.

Overall, this study discovered a new chemical space of highly active selenium-containing anticancer agents, worthy of being studied more in-depth in order to improve drug-likeness and to reveal the precise mode of action. In this context, compound **6**, as the most active agent

found in this study, will serve as a new lead structure for further pharmacomodulations and extended mechanistic studies as well as a medicinal chemistry optimization.

## 4. Experimental

### 4.1. Chemistry

Reagents were bought from Alfa Aesar (Karlsruhe, Germany) or Sigma Aldrich (Darmstadt, Germany). Solvents were dried over calcium hydrochloride (toluene) or calcium oxide (methanol). Reaction progress was verified using Thin Layer Chromatography (TLC), which was carried out on 0.2 mm Merck silica gel 60 F254 plates. Spots were visualized by UV light or treatment with Dragendorff reagent. Melting points (mp) were determined using a MEL-TEMP II apparatus and are uncorrected. The $^1$H NMR and $^{13}$C NMR spectra were obtained on a Varian Mercury-VX 300 MHz spectrometer and for the $^{77}$Se NMR on a Bruker Variance 500MHz spectrometer in DMSO-$d_6$, CDCl$_3$-$d$, MeOD-$d4$, or Acetone-$d_6$. Chemical shifts in the relative NMR spectra were reported in parts per million (ppm) on the δ scale using the solvent signal as an internal standard. Data are reported as follows: chemical shift, multiplicity (s, singlet; br. s, broad singlet; d, doublet; t, triplet; dd, doublet of doublet, q, quintet, td triplet of doublet, m, multiplet),), coupling constant *J* in Hertz (Hz), number of protons, proton's position (Ph-phenyl, Flou-Flourine, Pp-piperazine). LC-MS were carried out on a system consisting of a Waters Acquity UPLC, coupled to a Waters TQD mass spectrometer. Retention times ($t_R$) are given in minutes. The UPLC/MS purity of all final compounds was determined (%). The intermediates **18-20** are described in our previous works. [14, 21, 22] While the intermediates **21, 23, 25-30** were obtained according to the procedure described earlier [21] and are known in the literature [24, 26-29, 44, 45] (for details see Supporting Information).

### 4.1.1. General procedure for the Se-alkylation (5-14)

As part of this general procedure, the appropriate diphenyl diselenide (9.5 mmol) was dissolved in a 1:1 mixture of water and THF (50 mL) under protective nitrogen gas. Then, sodium borohydride (47.5 mmol) was added, and the mixture was stirred for approximately 35 minutes, with a decolourization of the solution observed already after 1-3 minutes. Next, a solution of hydantoin substitutions or piperazine derivatives (19.37 mmol) in THF or DCM (5 mL) was slowly added, and the reaction mixture was stirred at room temperature and monitored *via* TLC until the complete consumption of the starting material which occurred

after 24-48 hours. Upon completion, the reaction was quenched with 50 mL of a saturated aqueous solution of ammonium chloride and extracted with diethyl ether. The combined organic layers were dried over sodium sulphate and evaporated under reduced pressure to yield the desired products **5-14**.

### 4.1.1.1. Methyl 2-(2,5-dioxo-4,4-diphenyl-3-(4-(phenylselanyl)butyl)imidazolidin-1-yl)acetate (5)

Compound **18** (10 mmol) was used. White solid, mp 128°C. Yield 23.59%. LC/MS$^+$/: purity: 100 %, $t_R$=8.97, (ESI) $m/z$ [M+H]$^+$ 537.33. $C_{28}H_{28}O_4N_2Se$ (MW 536.12). $^1$H NMR (DMSO) δ 7.47–7.43 (m, 5H-Ph), 7.29 (s, 10H-2Ph), 4.34 (s, 2H-CH$_2$), 3.71 (s, 3H-CH$_3$), 3.33–3.28 (m, 2H-CH$_2$), 2.62 (t, $J$ = 7.3 Hz, 2H-CH$_2$), 1.37–1.17 (m, 2H-CH$_2$), 0.88 (dt, $J$ = 15.3, 7.7 Hz, 2H-CH$_2$). $^{13}$C NMR (DMSO) δ 172.80, 167.95, 136.69, 131.32, 129.15, 128.93, 128.79, 128.15, 128.07, 126.44, 74.51, 73.31, 52.55, 27.61, 26.47, 26.01. $^{77}$Se NMR (CDCL$_3$) δ 294.61.

### 4.1.1.2. Methyl 2-(2,5-dioxo-4,4-diphenyl-3-(6-(phenylselanyl)hexyl)imidazolidin-1-yl)acetate (6)

Compound **19,** Cas Number (1350707-01-5) (10 mmol) was used. Yellowish solid, mp 80°C. Yield 23.20%. $C_{30}H_{32}O_4N_2Se$ (MW 564.15). LC/MS$^+$/: purity: 92.76%, $t_R$=9.65, (ESI) $m/z$ [M+H]$^+$ 565.25. $^1$H NMR (CDCl$_3$) δ 7.31–7.27 (m, 2H-Ph), 7.26–7.18 (m, 10H-2Ph), 7.12–7.04 (m, 3H-Ph), 4.17 (s, 2H-CH$_2$), 3.64 (s, 3H-CH$_3$), 3.20–3.14 (m, 2H-CH$_2$), 2.62 (t, $J$ = 7.5 Hz, 2H-CH$_2$), 1.44 (s, 2H-CH$_2$), 1.36–1.28 (m, 2H-CH$_2$), 0.97 (dt, $J$ = 14.9, 7.5 Hz, 2H-CH$_2$), 0.83 (dt, $J$ = 14.6, 7.3 Hz, 2H-CH$_2$), 0.72 (dt, $J$ = 15.0, 7.5 Hz, 2H-CH$_2$). $^{13}$C NMR (CDCl$_3$) δ 173.57, 167.70, 154.88, 136.93, 132.30, 130.56, 128.99, 128.96, 128.79, 128.46, 126.59, 77.26, 77.01, 76.75, 75.25, 52.70, 42.13, 39.84, 33.59, 32.25, 29.69, 28.96, 27.60, 27.57, 26.03. $^{77}$Se NMR (CDCL$_3$) δ 290.63.

### 4.1.1.3. 1'-Methyl-3'-(4-(phenylselanyl)butyl)spiro[fluorene-9,4'-imidazolidine]-2',5'-dione (7)

Compound **20** (10 mmol) was used. White solid, mp 132°C. Yield 15.20%. $C_{26}H_{24}O_2N_2Se$ (MW 476.10). LC/MS$^+$/: purity: 95.87%, $t_R$=8.56, (ESI) $m/z$ [M+H]$^+$ 477.18. $^1$H NMR

(CDCl$_3$) δ 7.72 (d, $J$ = 7.6 Hz, 2H-Flu), 7.45 (td, $J$ = 7.5, 1.1 Hz, 2H- Flu), 7.36–7.31 (m, 2H-Flou), 7.28 (td, $J$ = 7.5, 1.0 Hz, 2H- Flu), 7.21 (d, $J$ = 7.5 Hz, 2H- Ph), 7.20–7.17 (m, 3H-Ph), 3.17 (s, 3H-CH$_3$), 2.96 (t, $J$ = 7.4 Hz, 2H-CH$_2$), 2.66–2.55 (m, 2H-CH$_2$), 1.44 (dt, $J$ = 15.1, 7.5 Hz, 2H-CH$_2$), 1.20 (dt, $J$ = 15.0, 7.5 Hz, 2H-CH$_2$). $^{13}$C NMR (CDCl$_3$) δ 171.89, 157.27, 141.52, 140.17, 132.64, 130.31, 129.85, 128.83, 128.24, 126.71, 123.57, 120.89, 77.16, 76.91, 76.65, 75.01, 40.63, 28.83, 26.87, 26.83, 25.61. $^{77}$Se NMR (CDCL$_3$) δ 292.63.

### 4.1.1.4. 1-Phenyl-4-(3-(phenylselanyl)propyl)piperazine (8)

Compound **21** (10 mmol), CAS Number (10599-17-4), was used. White solid, mp 248˚C. Yield 20.11%. C$_{19}$H$_{24}$N$_2$Se (MW 360.11). LC/MS$^+$/: purity: 100%, t$_R$=4.82, (ESI) $m/z$ [M+H]$^+$ 361.07. $^1$H NMR (MeOD) δ 7.61–7.58 (m, 2H-Ph), 7.34–7.28 (m, 5H-Ph), 7.05–7.02 (m, 2H-Ph), 6.94 (ddd, $J$ = 8.3, 2.0, 1.0 Hz, 1H-Ph), 3.79–3.37 (m, 8H-Pp-2,6-H+ Pp-3,5-H), 3.36 (s, 2H-CH$_2$), 3.05 (t, $J$ = 7.1 Hz, 2H-CH$_2$), 2.24–2.16 (m, 2H-CH$_2$). $^{13}$C NMR (DMSO) δ 149.57, 131.56, 129.57, 129.32, 129.07, 126.75, 119.88, 115.87, 55.10, 50.65, 45.21, 42.46, 23.74, 23.32. $^{77}$Se NMR (DMSO): 283.99.

### 4.1.1.5. 1-(2-Methoxyphenyl)-4-(3-(phenylselanyl)propyl)piperazine hydrochloride(9)

Commercial 1-(3-chloropropyl)-4-(2-methoxyphenyl)piperazine (10 mmol), CAS Number (21279-77-6), was used. White solid, mp 287˚C. Yield 8.6%. Basic form C$_{20}$H$_{26}$ON$_2$Se (MW 390.12), C$_{20}$H$_{27}$ClON$_2$Se (MW 426.10). LC/MS$^+$/: purity: 100%, t$_R$=4.97, (ESI) $m/z$ [M+H]$^+$ 391.17. $^1$H NMR (DMSO) δ 11.36 (s, 1H, NH$^+$), 7.23–7.15 (m, 6H-Ph), 6.91 (d, $J$ = 8.4 Hz, 2H-Ph), 6.78 (t, $J$ = 7.3 Hz, 1H-Ph), 3.69 (dd, $J$ = 11.7, 5.3 Hz, 2H-CH$_2$), 3.43 (d, $J$ = 10.3 Hz, 2H-CH$_2$), 3.16–2.96 (m, 8H-Pp-2,6-H+ Pp-3,5-H), 2.10–2.02 (m, 2H-CH$_2$). $^{13}$C NMR (126 MHz, DMSO) δ 131.58, 129.59, 129.41, 129.31, 129.08, 126.76, 115.86, 50.58, 45.19, 23.74, 23.31, 0.10. $^{77}$Se NMR (DMSO): 481.64.

### 4.1.1.6. 1-(4-Fluorophenyl)-4-(3-(phenylselanyl)propyl)piperazine hydrochloride (10):

Compound **21** (10 mmol), was used. White solid, mp 204˚C. Yield 37.68%. Basic form C$_{19}$H$_{23}$FN$_2$Se (MW 378.10), C$_{19}$H$_{24}$ClFN$_2$Se (MW 414.08). LC/MS$^+$/: purity: 100%, t$_R$=4.83, (ESI) $m/z$ [M+H]$^+$ 379.14. $^1$H NMR (DMSO) δ 11.10 (s, 1H, NH$^+$), 7.50–7.46 (m, 2H-Ph), 7.31–7.21 (m, 3H-Ph), 7.08–7.02 (m, 2H-Ph), 6.99-6.94 (m, 2H-Ph), 3.65 (d, $J$ = 10.3 Hz,2H-CH$_2$ ), 3.47 (d, $J$ = 9.8 Hz, 2H-CH$_2$), 3.20–2.96 (m, 8H-Pp-2,6-H+ Pp-3,5-H), 2.08 (dt, $J$ =

15.2, 7.5 Hz,2H-CH$_2$). $^{13}$C NMR (DMSO) δ 164.50, 157.51, 155.63, 146.41, 131.63, 129.55, 129.34, 126.82, 117.84, 117.78, 115.58, 115.40, 55.17, 50.72, 46.06, 23.85, 23.22. $^{77}$Se NMR (DMSO): 285.00.

### 4.1.1.7. 1-(3,4-Dichlorophenyl)-4-(3-(phenylselanyl)propyl)piperazine hydrochloride (11):

Commercial 1-(3-chloropropyl)-4-(3,4-dichlorophenyl)piperazine (10 mmol), CAS Number (101364-27-6), was used. White solid, mp 170˚C. Yield 15.09%. Basic form C$_{19}$H$_{22}$Cl$_2$N$_2$Se (MW 428.03), C$_{19}$H$_{23}$Cl$_3$N$_2$Se (MW 464.01). LC/MS$^+$/: purity: 99.22%, t$_R$=5.84, (ESI) *m/z* [M+H]$^+$ 429.12. $^1$H NMR (DMSO) δ 11.31 (s, 1H, NH$^+$), 7.55–7.48 (m, 2H, Ph), 7.44 (d, *J* = 9.0 Hz, 1H, Ph), 7.35–7.20 (m, 4H, Ph), 6.99 (dd, *J* = 9.0, 2.9 Hz, 1H, Ph), 3.86 (d, *J* = 13.2 Hz, 2H, CH$_2$), 3.48 (d, *J* = 11.7 Hz, 2H, CH$_2$), 3.28–3.16 (m, 4H, Pp-2,6-H), 3.12–2.98 (m, 4H, Pp-3,5-H), 2.11 (p, *J* = 7.5 Hz, 2H, CH$_2$). $^{13}$C NMR (DMSO) δ 149.28, 131.65, 131.61, 131.57, 130.63, 129.59, 129.33, 126.79, 120.75, 116.96, 115.79, 55.15, 50.22, 44.65, 23.75, 23.30. $^{77}$Se NMR (DMSO): 284.24.

### 4.1.1.8. 1-Methyl-4-(3-(phenylselanyl)propyl)piperazine hydrochloride (12):

Commercial 1-(3-chloropropyl)-4-methylpiperazine (10 mmol), CAS Number (104-16-5), was used. White solid, mp 132˚C. Basic form C$_{14}$H$_{22}$N$_2$Se (MW 298.09), C$_{14}$H$_{22}$ClN$_2$Se (MW 333.59). Yield 11.97%. LC/MS$^+$/: purity: 97.97%, t$_R$=2.89, (ESI) *m/z* [M+H]$^+$ 299.13. $^1$H NMR (DMSO) δ 12.01 (s, 1H, NH$^+$), 7.52–7.46 (m, 2H, Ph), 7.33–7.22 (m, 3H, Ph), 3.50–3.13 (m, 10H, 8H-Pp-2,6-H+ Pp-3,5-H+ 2H-CH$_2$), 3.01 (t, *J* = 7.4 Hz, 2H, CH$_2$), 2.81 (s, 3H, CH$_3$), 2.07 (p, *J* = 7.6 Hz, 2H). $^{13}$C NMR (DMSO) δ 131.47, 129.59, 129.34, 129.25, 126.74, 55.29, 49.39, 47.99, 23.89, 23.31, 23.05, 22.80. $^{77}$Se NMR (DMSO): 284.41.

### 4.1.1.9. Ethyl 4-(3-(phenylselanyl)propyl)piperazine-1-carboxylate hydrochloride (13):

Synthesis from 10 mmol of ester **26**. White solid, mp 83˚C. Yield 23.59%. Basic form C$_{16}$H$_{24}$N$_2$O$_2$Se (MW 356.10), C$_{16}$H$_{24}$ClN$_2$O$_2$Se (MW 391.60). LC/MS$^+$/: purity: 98.59%, t$_R$=3.82, (ESI) *m/z* [M+H]$^+$ 357.21. $^1$H NMR (DMSO) δ 11.62 (s, 1H, NH$^+$), 7.53–7.48 (br, 2H), 7.33–7.23 (m, 3H, Ph), 4.06 (m, 2H, Ph), 4.00 (d, *J* = 13.4 Hz, 2H, CH$_2$), 3.39 (d, *J* = 9.8 Hz, 4H, Pp-2,6-H), 3.18–3.11 (m, 2H, CH$_2$), 3.04–2.91 (m, 4H, Pp-3,5-H), 2.08 (p, *J* = 7.5

Hz, 2H), 1.18 (t, $J$ = 7.1 Hz, 3H). $^{13}$C NMR (DMSO) δ 154.27, 131.65, 131.60, 131.56, 129.57, 129.31, 126.76, 61.31, 55.27, 50.31, 23.66, 23.29, 14.47. $^{77}$Se NMR (DMSO) δ 283.96.

### 4.1.2. General procedure of synthesis of 1,3,5-triazines (14-17)

Sodium (10 mmol) was dissolved in 10 mL of absolute methanol, then 4-methylpiperazin-1-yl biguanidine x 2HCl (5 mmol) and the appropriate carboxylic acid ester (5 mmol) were added. The reaction mixture was refluxed for 15-30 h. After cooling to room temperature, water (10 mL) was added and the mixture was stirred for 0.5 h. The precipitated triazine product was separated and crystallized from methanol.

### 4.1.2.1. 4-(4-Methylpiperazin-1-yl)-6-((phenylselanyl)methyl)-1,3,5-triazin-2-amine hydrochloride (14):

Synthesis from 10 mmol of ester **27**. White solid. Yield 26%, mp 249°C. Basic form $C_{15}H_{20}N_6Se$ (MW 364.09), $C_{15}H_{20}ClN_6Se$ (MW 400.07). LC/MS$^+$: purity: 100%, $t_R$=2.82, (ESI) m/z [M+H]$^+$ 365.12. $^1$H-NMR (DMSO) δ 11.50 (s, 1H-NH$^+$), 7.87 (br.s. 2H-NH$_2$), 7.61–7.56 (m, 2H Ph), 7.37–7.25 (m, 3H Ph), 3.96 (d, $J$=5.4 Hz, 2H-CH$_2$), 3.50–2.78 (m, 8H, 4H-Pp-2,6-H+4H-Pp-3,5-H), 2.73 (d, $J$ = 4.0 Hz, 3H-CH$_3$). $^{13}$C-NMR (DMSO) δ 175.48, 171.16, 167.35, 164.82, 134.10, 131.78, 131.40, 130.45, 129.49, 129.25, 127.03, 125.59, 54.77, 46.23, 42.84, 34.62, 33.19.

### 4.1.2.2. 4-(4-Methylpiperazin-1-yl)-6-(1-(phenylselanyl)ethyl)-1,3,5-triazin-2-amine hydrochloride (15) :

Synthesis from 10 mmol of ester **28**. White solid. Yield 12.19%, mp 238°C. Basic form $C_{16}H_{22}N_6Se$ (MW 378.11), $C_{16}H_{23}ClN_6Se$ (MW 413.81). LC/MS$^+$/: purity: 100%, $t_R$=3.23, (ESI) m/z [M+H]$^+$ 379.08. $^1$H-NMR (DMSO) δ 11.93 (s, 1H-NH$^+$), 8.33 (br.s, 2H-NH$_2$), 7.54 (dt, $J$ = 7.0, 1.4 Hz, 2H-Ph), 7.45–7.29 (m, 3H-Ph), 4.34 (q, $J$ = 7.0 Hz, 1H-CH), 4.11–2.55 (m, 11H, 4H-Pp-2,6-H + 4H-Pp-3,5-H + 3H-Pp-CH$_3$), 1.59 (s, 3H-CH$_3$). $^{13}$C-NMR (DMSO) δ 162.20, 136.14, 131.33, 129.98, 129.64, 129.22, 128.34, 51.62, 42.38, 18.15. $^{77}$Se NMR (DMSO) δ 492.76.

### 4.1.2.3 4-(4-Methylpiperazin-1-yl)-6-(1-(phenylselanyl)propyl)-1,3,5-triazin-2-amine hydrochloride (16)

Synthesis from 10 mmol of ester **29** White solid. Yield 29.78%, mp 231˚C. Basic form $C_{17}H_{24}N_6Se$ (MW 392.12), $C_{17}H_{25}ClN_6Se$ (MW 428.10). LC/MS$^{+/}$: purity: 100%, $t_R$=3.67, (ESI) *m/z* [M+H]$^+$ 393.17. $^1$H NMR (DMSO) δ 11.87 (s, 1H, NH$^+$), 9.02–7.87 (br, 2H, NH$_2$), 7.56–7.50 (m, 2H, Ph), 7.42–7.30 (m, 3H, Ph), 4.07 (t, *J* = 7.6 Hz, 1H, CH), 3.54–2.93 (m, 8H, Pp-2,6-H+ Pp-3,5-H), 2.75 (s, 3H, CH$_3$), 1.94 (d, *J* = 76.0 Hz, 2H, CH$_2$), 0.95 (t, *J* = 7.2 Hz, 3H, CH$_3$). $^{13}$C NMR (DMSO) δ 167.12, 164.46, 162.05, 135.95, 131.30, 130.45, 129.97, 129.64, 129.19, 128.32, 51.89, 42.44, 42.37, 28.93, 25.05, 21.87, 13.76, 12.82, 11.32. $^{77}$Se NMR (DMSO) δ 454.52.

### 4.1.2.4.    4-(4-Methylpiperazin-1-yl)-6-(2-(phenylselanyl)propan-2-yl)-1,3,5-triazin-2-amine hydrochloride (17)

Synthesis from 10 mmol of ester **30**. Light yellow solid. Yield 12.19%, mp 252˚C. Basic form $C_{17}H_{24}N_6Se$ (MW 392.12), $C_{17}H_{25}ClN_6Se$ (MW 428.10). LC/MS$^{+/}$: purity: 96.21%, $t_R$=3.72, (ESI) *m/z* [M+H]$^+$ 393.10. $^1$H NMR (DMSO) δ 11.45 (br, 1H, NH$^+$), 8.83–7.75 (br, 2H, NH$_2$), 7.61–7.41 (m, 3H, Ph), 7.39–7.33 (m, 2H, Ph), 3.36–2.86 (m, 8H, Pp-2,6-H+ Pp-3,5-H), 2.76 (s, 3H, CH$_3$), 1.69 (s, 6H, 2CH$_3$). $^{13}$C NMR (DMSO) δ 174.94, 162.37, 162.09, 157.22, 132.42, 131.30, 130.45, 129.96, 128.31, 71.57, 51.88, 51.54, 42.41, 42.36, 28.81, 27.59, 18.71. $^{77}$Se NMR (DMSO) δ 447.73.

### 4.2. Biological assays
### 4.2.1. Assays in mouse T-lymphoma
### Cell lines

The L5178Y mouse T-cell lymphoma cells (ECACC Cat. No. 87111908, obtained from FDA, Silver Spring, MD, USA) were transfected with pHa MDR1/A retrovirus. The *ABCB1*-expressing cell line (MDR) was selected by culturing the infected cells with colchicine. L5178Y (parental, PAR) mouse T-cell lymphoma cells and the L5178Y human *ABCB1*-transfected subline were cultured in McCoy's 5A medium supplemented with 10% heat-inactivated horse serum, 200 mM L-glutamine, and penicillin-streptomycin mixture in 100 U/l and 10 mg/l concentration, respectively.

### Assay for cytotoxic effect in mouse lymphoma cells

Stock solutions of compounds were 10 mM in DMSO. The effects of increasing concentrations of the drugs alone on cell growth were tested in 96-well flat-bottomed

microtiter plates. The compounds were diluted in 100 µL of McCoy's 5A medium. $1 \times 10^4$ mouse T-cell lymphoma cells (PAR or MDR) in 100 µL of medium were then added to each well, with the exception of the medium control wells. The culture plates were further incubated at 37 ºC for 24 h; at the end of the incubation period, 20 µL of MTT solution (from a 5 mg/mL stock) was added to each well. After incubation at 37 ºC for 4 h, 100 µL of SDS solution (10% in 0.01 M HCI) was added to each well, and the plates were further incubated at 37 ºC overnight. The cell growth was determined by measuring the OD at 540 nm (ref. 630 nm) with a Multiscan EX ELISA reader (Thermo Labsystems, Cheshire, WA, USA). $IC_{50}$ values were calculated *via* the following equation:

$$100 - \left[ \frac{OD_{sample} - OD_{medium\ control}}{OD_{cell\ control} - OD_{medium\ control}} \right] \times 100$$

*Assay for antiproliferative effect in mouse lymphoma cells*

The effects of increasing concentrations of the drugs alone on cell growth were tested in 96-well flat-bottomed microtiter plates. The compounds were diluted in 100 µL of McCoy's 5A medium. $6 \times 10^3$ mouse T-cell lymphoma cells (PAR or MDR) in 100 µL of medium were then added to each well, with the exception of the medium control wells. The culture plates were further incubated at 37 ºC for 72 h in a $CO_2$ incubator; at the end of the incubation period, 20 µL of MTT solution (from a 5 mg/mL stock) was added to each well. After incubation at 37 ºC for 4 h, 100 µL of SDS solution (10% in 0.01 M HCI) was added to each well, and the plates were further incubated at 37 ºC overnight. The cell growth was determined by measuring the OD at 540 nm (ref. 630 nm) with a Multiscan EX ELISA reader (Thermo Labsystems, Cheshire, WA, USA). $IC_{50}$ values were calculated *via* the following equation:

$$100 - \left[ \frac{OD_{sample} - OD_{medium\ control}}{OD_{cell\ control} - OD_{medium\ control}} \right] \times 100$$

*Fluorescence uptake assay*

The cell numbers of the L5178Y PAR and MDR cell lines were adjusted to $2 \times 10^6$ cells/mL, resuspended in serum-free McCoy's 5A medium, and distributed in 0.5 mL aliquots into Eppendorf centrifuge tubes. The tested compounds were added at a final concentration of 0.2, 2, or 20 µM, and the samples were incubated for 10 min at room temperature. Verapamil was applied as a positive control at 20 µM. DMSO was added to the negative control tubes in the same volume as had been used for the tested compounds. No activity of DMSO was observed. Next, 10 µL (5.2 µM final concentration) of the fluorochrome and ABCB1 substrate rhodamine 123 was added to the samples, and the cells were incubated for a further 20 min at 37 ºC, washed twice and re-suspended in 1 mL PBS for analysis. The fluorescence of the cell population was measured with a PartecCyFlow®flow cytometer (Partec, Münster, Germany). The percentage of mean fluorescence intensity was calculated for the treated MDR cells as compared with the untreated cells. A fluorescence activity ratio (FAR) was calculated based on the measured fluorescence values *via* the following equation:

$$FAR = \frac{MDR_{treated}/MDR_{control}}{parental_{treated}/parental_{control}}$$

### 4.2.2. Assays with JURKAT human T-lymphocytes
*Cell culture and treatments*
JURKAT human T lymphocyte cells (ATCC, VA, USA) were propagated in RPMI 1640 medium (Gibco, Monza, Italy) with 10% fetal bovine serum (FBS; Gibco, Monza, Italy), 2mML-glutamine (Euroclone, Pero (MI), Italy), and antibiotics (100 U/mL penicillin, 100 g/mL streptomycin) (Euroclone, Pero (MI), Italy).

For the treatments with compound **6**, doxorubicin and DMSO as a negative control, cells were seeded and treated once with compound **6** at the final concentration of 0,1µM, 0,5 µM and 2 µM, alone or in combination with doxorubicin at the final concentration of 50 nM and 250 nM. Cells were collected after 24 and /or 72 hours from the treatment and analysed for proliferation rate and gene expression.

*RNA extraction, reverse transcription, and quantitative PCR in JURKAT cells*
RNAs were extracted by ReliaPrep™ RNA Tissue Miniprep (Promega, Madison, WI, USA) and reverse-transcribed with PrimeScript RT Master Mix (Takara, Kusatsu, Shiga, Japan). cDNAs were amplified by a qPCR reaction using GoTaq qPCR Master Mix (Promega) and analyzed with the oligonucleotide pairs specific for the target genes. Relative amounts,

determined with the 2(−ΔCt) method, were normalized with respect to the human housekeeping gene L32.

The primers used are as follows: L32 (forward: 5′-GGAGCGACTGCTACGGAAG-3′, reverse: 5′-GATACTGTCCAAAAGGCTGGAA-3′), CyclinD1 (forward: 5'-CCTCTAAGATGAAGGAGACCA-3′, reverse: 5′-CACTTGAGCTTGTTCACCA-3′), and p53 (forward: 5′-GGCCCACTTCACCGTACTAA-3′, reverse: 5′-GTGGTTTCAAGGCCAGATGT-3′).

*Cell proliferation assay*

Cell viability was measured using a CellTiter 96® AQueous One Solution Cell Proliferation Assay (MTS) (Promega) following the manufacturer's instructions, as reported in Stazi et al., 2019 [46]. Briefly, JURKAT cells were seeded in 96 well tissue culture plates. After 24 h or 72 h of treatment with compound **6**, doxorubicin, or DMSO as a negative control at the reported concentrations, 20 μL of AQueous One Solution Reagent was added to each well and absorbance was recorded at 490 nm. Three independent experiments were performed.

*Statistical methods*

Statistical analysis was performed using Statistica v10 software (StatSoft, USA). The correlation coefficients ($r$, $r^2$), and the standard errors of the slope, interception, and estimate ($S_a$, $S_b$, $S_e$) were used as the basis for testing the linearity of regression plots.

Statistical significance for gene expression analysis and proliferation assays was determined with a t-test with GraphPad Prism version 5.0 (La Jolla, CA, USA). Differences were considered significant at $P < 0.05$ (*$p < 0.05$; **$p < 0.01$; ***$p < 0.001$).

*4.2.3. Assays with human neuroblastoma cell line SH-SY5Y*
*Cell culture and treatment conditions*

Human neuroblastoma cell line SH-SY5Y (*ATCC*® no. CRL-2266™) was grown in Dulbecco's Modified Eagle's Medium/Nutrient Mixture F-12 (DMEM/F12, Life Technologies) with 10% (v/v) fetal bovine serum (FBS, South America, Life Technologies) at 37°C in a humidified atmosphere of 5% $CO_2$/95% air. Cells were routinely passaged at 70% confluence by trypsinization (0.05% Trypsin-EDTA, Invitrogen) and re-seeded at 5 x $10^3$ cells/cm$^2$. To make experiments comparable, cells at passages 10-17 were evaluated. In every experiment, cells were seeded in 100 μl (96-well plates) of complete growth medium and

initially cultured for 24h. Subsequently, the medium was changed to medium containing tested compounds diluted to the desired concentrations. After 72h, the given assay was performed as described below. All tested compounds were dissolved in DMSO to generate 10 mM stock. Directly before analysis, each stock solution of tested compounds was made in DMSO as a 1000-fold stock solution and then diluted in culture medium to a final desired concentration.

*Cell viability assay*

SH-SY5Y cells ($2.5 \times 10^4$ cells/well) were cultured in transparent 96-well plates (*Nunc*) in DMEM/F12 supplemented with 10% FBS in the presence of dimethylsulfoxide (DMSO < 0.1%, vehicle control) or increasing concentration of compounds **5, 6** and **7** (0.1, 0.5, 2, 10 [μM]). Treatment with compounds was performed for 72 h. After the incubation time, cell viability was examined using an MTS-based [3-(4,5-dimethylthiazol-2-yl)-5-(3-carboxymethoxyphenyl)-2-(4-sulfophenyl)-2 H tetrazolium] CellTiter96® AQueous One Solution Cell Proliferation Assay (Promega, Madison, USA) following the manufacturer's protocol. Briefly, 20 μl of MTS solution was pipetted into each well containing 100 μl of culture or culture medium (negative control) and incubated at 37°C for 4 h. After incubation time, formazan product turnover absorbance was measured at 490 nm using the microplate reader EnSpire (PerkinElmer, Massachusetts, USA).

*Statistical analysis*

Data are presented as the mean ± SEM of two independent experiments. Each treatment point was repeated (six times) in two technical and independent replicates. All statistical analyses were carried out using GraphPad Prism 7 with significance determined by One-way ANOVA followed by Bonferroni's post-hoc comparisons tests as detailed in the figure legends.

*4.2.4. Intrinsic activity towards Pgp in vitro*

The luminescent Pgp-Glo™ Assay System used for determination of 1,3,5-Triazine selenium derivatives influence on P-gp activity was purchased from Promega (Madison, WI, USA). The assay was performed in triplicate, as described previously [33-35]. Compounds **5-7** (100 μM) were incubated with Pgp membranes for 40 minutes at 37 °C. The references: Pgp-stimulator verapamil (VER) and Pgp-negative compound caffeine (CFN) were incubated at 200 and 100 μM, respectively. For basal P-gp activity calculation, the membranes were

incubated with 100 µM of sodium orthovanadate ($Na_3VO_4$). The luminescence signal was measured by microplate reader EnSpire PerkinElmer (Waltham, MA, USA). The statistical significances were calculated using GraphPad Prism 8.0.1 software.

## 4.3. Lipophilicity study

*Thin-Layer Chromatography*

The mobile phases were prepared by mixing the respective amounts of water and organic modifier (methanol) in a range from 40 to 90% (v/v) in 5% increments. TLC was carried out on Silica gel 60 RP-18 $F_{254}$ plates (7×10 cm) plates (Merck, Darmstadt, Germany). Methanol was used to prepare the solutions of the substances. Solutions (10 µL) of the analysed compounds were applied to the plates as 5 mm bands, 10 mm apart, and 10 mm from the lower edge and sides of the plates, by using a Linomat V applicator (Camag, Basel, Switzerland). The vertical chamber (Sigma–Aldrich, St. Louis, USA), 20×10×18 cm in size, was saturated with the mobile phase for 20 min. The development was carried out over 9 cm from the starting line at a temperature of 20°C. Next, the plates were dried at room temperature, and the spots were observed in ultraviolet light at 254 and/or 366 nm (UV lamp, Camag, Basel, Switzerland). In each case, sharp and symmetric spots without a tendency for tailing were obtained. Each experiment was run in triplicate, and mean $R_F$ (retardation factor) values were calculated.

Starting from the $R_F$ values, the $R_M$ parameters were computed as described in the formula:

$R_M = \log(1/R_F - 1)$

Linear correlations between the $R_M$ values of the substances and the concentration of organic modifier in mobile phases were calculated for each compound with the Soczewiński-Wachtmeister equation [47].

$R_M = R_{M0} + aC$ where $C$ is the concentration of the organic solvent (in %) in the mobile phase, $a$ is the slope, and $R_{M0}$ is the concentration of organic modifier extrapolated to zero.

## 4.4. Metabolic stability assay

The *in vitro* evaluation of metabolic pathways was performed by 120 min incubation of compounds **5-7** at 37° C with mouse liver microsomes (MLMs) obtained from Sigma-Aldrich (St. Louis, MO, USA), according to the described previously protocols [48, 49]. The LC/MS analyses with additional MS ion fragmentation of the products and substrates were performed to determine the most probable structures of metabolites.

## 4.5. Drug-drug interaction prediction

The used CYP3A4 P450-Glo[TM] commercial assay was purchased from Promega (Madison, WI, USA). The influence of compounds on CYP3A4 activity was tested according to the manufacturer protocol and as described previously [48, 49]. The bioluminescence signal was measured with a microplate reader EnSpire (Perkin Elmer, Waltham, MA, USA) in luminescence mode.

## Supporting Information

In the supporting information available online at XXX, we provide the detailed procedures for the preparation of the compounds **21-30**, copies of the NMR spectra $^1$H, $^{13}$C, $^{77}$Se and LCMS data for **5-17**, lipophilicity data for compounds **5-17** by RP-TLC and the ion fragment analyses and the most probable structures of compounds **5, 6, 7** during our metabolic stability tests.

## Acknowledgements

## References

[1] S. Nobili, I. Landini, B. Giglioni, E. Mini, Pharmacological strategies for overcoming multidrug resistance, Curr Drug Targets, 7 (2006) 861-879.

[2] A.A. Stavrovskaya, T.P. Stromskaya, Transport proteins of the ABC family and multidrug resistance of tumor cells, Biochemistry (Mosc), 73 (2008) 592-604.

[3] E. Teodori, S. Dei, S. Scapecchi, F. Gualtieri, The medicinal chemistry of multidrug resistance (MDR) reversing drugs, Farmaco, 57 (2002) 385-415.

[4] R. Ernst, P. Kueppers, J. Stindt, K. Kuchler, L. Schmitt, Multidrug efflux pumps: substrate selection in ATP-binding cassette multidrug efflux pumps--first come, first served?, FEBS J, 277 (2010) 540-549.

[5] M.D. Hall, M.D. Handley, M.M. Gottesman, Is resistance useless? Multidrug resistance and collateral sensitivity, Trends Pharmacol Sci, 30 (2009) 546-556.

[6] X. Liu, ABC Family Transporters, Adv Exp Med Biol, 1141 (2019) 13-100.

[7] I. Genovese, A. Ilari, Y.G. Assaraf, F. Fazi, G. Colotti, Not only P-glycoprotein: Amplification of the ABCB1-containing chromosome region 7q21 confers multidrug resistance upon cancer cells by coordinated overexpression of an assortment of resistance-related proteins, Drug Resist Updat, 32 (2017) 23-46.

[8] H. Hamada, T. Tsuruo, Functional role for the 170- to 180-kDa glycoprotein specific to drug-resistant tumor cells as revealed by monoclonal antibodies, Proc Natl Acad Sci U S A, 83 (1986) 7785-7789.

[9] Y. Tanigawara, N. Okamura, M. Hirai, M. Yasuhara, K. Ueda, N. Kioka, T. Komano, R. Hori, Transport of digoxin by human P-glycoprotein expressed in a porcine kidney epithelial cell line (LLC-PK1), J Pharmacol Exp Ther, 263 (1992) 840-845.

[10] G. Spengler, M. Gajdacs, M.A. Marc, E. Dominguez-Alvarez, C. Sanmartin, Organoselenium Compounds as Novel Adjuvants of Chemotherapy Drugs-A Promising Approach to Fight Cancer Drug Resistance, Molecules, 24 (2019).

[11] K. Katayama, K. Noguchi, Y. Sugimoto, Regulations of P-glycoprotein/ABCB1/MDR1 in human cancer cells, New Journal of Science, 2014 (2014).

[12] G. Spengler, J. Handzlik, I. Ocsovszki, M. Viveiros, K. Kiec-Kononowicz, J. Molnar, L. Amaral, Modulation of multidrug efflux pump activity by new hydantoin derivatives on colon adenocarcinoma cells without inducing apoptosis, Anticancer Res, 31 (2011) 3285-3288.

[13] A. Martins, A. Dymek, J. Handzlik, G. Spengler, A. Armada, J. Molnar, K. Kiec-Kononowicz, L. Amaral, Activity of fourteen new hydantoin compounds on the human ABCB1 efflux pump, In Vivo, 26 (2012) 293-297.

[14] E. Zeslawska, A. Kincses, G. Spengler, W. Nitek, K. Wyrzuc, K. Kiec-Kononowicz, J. Handzlik, The 5-aromatic hydantoin-3-acetate derivatives as inhibitors of the tumour multidrug resistance efflux pump P-glycoprotein (ABCB1): Synthesis, crystallographic and biological studies, Bioorg Med Chem, 24 (2016) 2815-2822.

[15] E. Dominguez-Alvarez, M. Gajdacs, G. Spengler, J.A. Palop, M.A. Marc, K. Kiec-Kononowicz, L. Amaral, J. Molnar, C. Jacob, J. Handzlik, C. Sanmartin, Identification of selenocompounds with promising properties to reverse cancer multidrug resistance, Bioorg Med Chem Lett, 26 (2016) 2821-2824.

[16] N. Kerru, P. Singh, N. Koorbanally, R. Raj, V. Kumar, Recent advances (2015-2016) in anticancer hybrids, Eur J Med Chem, 142 (2017) 179-212.

[17] A. Makowska, F. Saczewski, P.J. Bednarski, J. Saczewski, L. Balewski, Hybrid Molecules Composed of 2,4-Diamino-1,3,5-triazines and 2-Imino-Coumarins and Coumarins. Synthesis and Cytotoxic Properties, Molecules, 23 (2018).

[18] P. Singla, V. Luxami, K. Paul, Synthesis and in vitro evaluation of novel triazine analogues as anticancer agents and their interaction studies with bovine serum albumin, Eur J Med Chem, 117 (2016) 59-69.

[19] M. Gajdacs, G. Spengler, C. Sanmartin, M.A. Marc, J. Handzlik, E. Dominguez-Alvarez, Selenoesters and selenoanhydrides as novel multidrug resistance reversing agents: A confirmation study in a colon cancer MDR cell line, Bioorg Med Chem Lett, 27 (2017) 797-802.

[20] B. Wu, J. Ge, Z. Zhang, C. Huang, X. Li, Z. Tan, X. Fang, J. Sun, Combination of Sodium Selenite and Doxorubicin Prodrug Ac-Phe-Lys-PABC-ADM Affects Gastric Cancer Cell Apoptosis in Xenografted Mice, BioMed research international, 2019 (2019) 2486783.

[21] J. Handzlik, M. Bajda, M. Zygmunt, D. Maciag, M. Dybala, M. Bednarski, B. Filipek, B. Malawska, K. Kiec-Kononowicz, Antiarrhythmic properties of phenylpiperazine derivatives of phenytoin with alpha(1)-adrenoceptor affinities, Bioorg Med Chem, 20 (2012) 2290-2303.

[22] J. Handzlik, E. Szymanska, J. Chevalier, E. Otrebska, K. Kiec-Kononowicz, J.M. Pages, S. Alibert, Amine-alkyl derivatives of hydantoin: new tool to combat resistant bacteria, Eur J Med Chem, 46 (2011) 5807-5816.

[23] W. Ali, M. Wiecek, D. Lazewska, R. Kurczab, M. Jastrzebska-Wiesek, G. Satala, K. Kucwaj-Brysz, A. Lubelska, M. Gluch-Lutwin, B. Mordyl, A. Siwek, M.J. Nasim, A. Partyka, S. Sudol, G. Latacz, A. Wesolowska, K. Kiec-Kononowicz, J. Handzlik, Synthesis and computer-aided SAR studies for derivatives of phenoxyalkyl-1,3,5-triazine as the new potent ligands for serotonin receptors 5-HT6, Eur J Med Chem, 178 (2019) 740-751.

[24] S.-J. Zhu, H.-Z. Ying, Y. Wu, N. Qiu, T. Liu, B. Yang, X.-W. Dong, Y.-Z. Hu, Design, synthesis and biological evaluation of novel podophyllotoxin derivatives bearing 4β-disulfide/trisulfide bond as cytotoxic agents, RSC Advances, 5 (2015) 103172-103183.

[25] D. Lazewska, R. Kurczab, M. Wiecek, K. Kaminska, G. Satala, M. Jastrzebska-Wiesek, A. Partyka, A.J. Bojarski, A. Wesolowska, K. Kiec-Kononowicz, J. Handzlik, The computer-aided discovery of novel family of the 5-HT6 serotonin receptor ligands among derivatives of 4-benzyl-1,3,5-triazine, Eur J Med Chem, 135 (2017) 117-124.

[26] S. Paudel, S. Acharya, K.M. Kim, S.H. Cheon, Design, synthesis, and biological evaluation of arylpiperazine-benzylpiperidines with dual serotonin and norepinephrine reuptake inhibitory activities, Bioorg Med Chem, 24 (2016) 2137-2145.

[27] P. Bernardelli, A. Denis, E. Lorthiois, H. Jacobelli, F. Vergne, D. Serradeil, F. Rousseau, A. Cronin, M. Kemp, Preparation of substituted phenols as histamine H3 ligands, in, Warner-Lambert Company LLC, USA . 2005, pp. 126 pp.

[28] S. Torii, T. Inokuchi, G. Asanuma, N. Sayo, H. Tanaka, A Direct Phenylselenenylation of Alkyl Halides, Alkenyl Sulfonates, and Epoxides by an Electroreduction of Diphenyl Diselenide, Chemistry Letters, 9 (1980) 867-868.

[29] F. Malihi, D.L. Clive, C.C. Chang, Minaruzzaman, Synthetic studies on CP-225,917 and CP-263,114: access to advanced tetracyclic systems by intramolecular conjugate displacement and [2,3]-Wittig rearrangement, J Org Chem, 78 (2013) 996-1013.

[30] M.M. Cornwell, I. Pastan, M.M. Gottesman, Certain calcium channel blockers bind specifically to multidrug-resistant human KB carcinoma membrane vesicles and inhibit drug binding to P-glycoprotein, J Biol Chem, 262 (1987) 2166-2170.

[31] G. Spengler, M. Viveiros, M. Martins, L. Rodrigues, A. Martins, J. Molnar, I. Couto, L. Amaral, Demonstration of the activity of P-glycoprotein by a semi-automated fluorometric method, Anticancer Res, 29 (2009) 2173-2177.

[32] G. Spengler, M. Evaristo, J. Handzlik, J. Serly, J. Molnar, M. Viveiros, K. Kiec-Kononowicz, L. Amaral, Biological activity of hydantoin derivatives on P-glycoprotein (ABCB1) of mouse lymphoma cells, Anticancer Res, 30 (2010) 4867-4871.

[33] G. Latacz, A. Lubelska, M. Jastrzebska-Wiesek, A. Partyka, A. Sobilo, A. Olejarz, K. Kucwaj-Brysz, G. Satala, A.J. Bojarski, A. Wesolowska, K. Kiec-Kononowicz, J. Handzlik, In the search for a lead structure

among series of potent and selective hydantoin 5-HT7 R agents: The drug-likeness in vitro study, Chem Biol Drug Des, 90 (2017) 1295-1306.

[34] G. Latacz, A. Lubelska, M. Jastrzebska-Wiesek, A. Partyka, K. Kucwaj-Brysz, A. Wesolowska, K. Kiec-Kononowicz, J. Handzlik, MF-8, a novel promising arylpiperazine-hydantoin based 5-HT7 receptor antagonist: In vitro drug-likeness studies and in vivo pharmacological evaluation, Bioorg Med Chem Lett, 28 (2018) 878-883.

[35] G. Latacz, A.S. Hogendorf, A. Hogendorf, A. Lubelska, J.M. Wieronska, M. Wozniak, P. Cieslik, K. Kiec-Kononowicz, J. Handzlik, A.J. Bojarski, Search for a 5-CT alternative. In vitro and in vivo evaluation of novel pharmacological tools: 3-(1-alkyl-1H-imidazol-5-yl)-1H-indole-5-carboxamides, low-basicity 5-HT7 receptor agonists, Medchemcomm, 9 (2018) 1882-1890.

[36] A.A. Mahbub, C.L. Le Maitre, S.L. Haywood-Small, N.A. Cross, N. Jordan-Mahy, Polyphenols act synergistically with doxorubicin and etoposide in leukaemia cell lines, Cell Death Discov, 1 (2015) 15043.

[37] A.A. Fernandez-Ramos, C. Marchetti-Laurent, V. Poindessous, S. Antonio, C. Petitgas, I. Ceballos-Picot, P. Laurent-Puig, S. Bortoli, M.A. Loriot, N. Pallet, A comprehensive characterization of the impact of mycophenolic acid on the metabolism of Jurkat T cells, Sci Rep, 7 (2017) 10550.

[38] A. Zuryn, A. Litwiniec, L. Gackowska, A. Pawlik, A.A. Grzanka, A. Grzanka, Expression of cyclin A, B1 and D1 after induction of cell cycle arrest in the Jurkat cell line exposed to doxorubicin, Cell Biol Int, 36 (2012) 1129-1135.

[39] H. Luo, Y. Yang, F. Huang, F. Li, Q. Jiang, K. Shi, C. Xu, Selenite induces apoptosis in colorectal cancer cells via AKT-mediated inhibition of beta-catenin survival axis, Cancer Lett, 315 (2012) 78-85.

[40] H. Zeng, W.H. Cheng, L.K. Johnson, Methylselenol, a selenium metabolite, modulates p53 pathway and inhibits the growth of colon cancer xenografts in Balb/c mice, J Nutr Biochem, 24 (2013) 776-780.

[41] D.S. Thakur, Topoisomerase II inhibitors in cancer treatment, Int J Pharm Sci Nanotechnol, 3 (2011) 1173-1181.

[42] O. Tacar, C.R. Dass, Doxorubicin-induced death in tumour cells and cardiomyocytes: is autophagy the key to improving future clinical outcomes?, J Pharm Pharmacol, 65 (2013) 1577-1589.

[43] B.J. Aubrey, G.L. Kelly, A. Janic, M.J. Herold, A. Strasser, How does p53 induce apoptosis and how does this relate to p53-mediated tumour suppression?, Cell death and differentiation, 25 (2018) 104-113.

[44] D.L. Clive, Z. Li, M. Yu, Intramolecular conjugate displacement: a general route to hexahydroquinolizines, hexahydroindolizines, and related [m,n,0]-bicyclic structures with nitrogen at a bridgehead, J Org Chem, 72 (2007) 5608-5617.

[45] Z. Janousek, S. Piettre, F. Gorissen-Hervens, H.G. Viehe, Capto-dative substituent effects, Journal of Organometallic Chemistry, 250 (1983) 197-202.

[46] G. Stazi, C. Battistelli, V. Piano, R. Mazzone, B. Marrocco, S. Marchese, S.M. Louie, C. Zwergel, L. Antonini, A. Patsilinakos, R. Ragno, M. Viviano, G. Sbardella, A. Ciogli, G. Fabrizi, R. Cirilli, R. Strippoli, A. Marchetti, M. Tripodi, D.K. Nomura, A. Mattevi, A. Mai, S. Valente, Development of alkyl glycerone phosphate synthase inhibitors: Structure-activity relationship and effects on ether lipids and epithelial-mesenchymal transition in cancer cells, Eur J Med Chem, 163 (2019) 722-735.

[47] E. Soczewiński, C.A. Wachtmeister, The relation between the composition of certain ternary two-phase solvent systems and RM values, Journal of Chromatography A, 7 (1962) 311-320.

[48] A. Lubelska, G. Latacz, M. Jastrzebska-Wiesek, M. Kotanska, R. Kurczab, A. Partyka, M.A. Marc, D. Wilczynska, A. Doroz-Plonka, D. Lazewska, A. Wesolowska, K. Kiec-Kononowicz, J. Handzlik, Are the Hydantoin-1,3,5-triazine 5-HT6R Ligands a Hope to a Find New Procognitive and Anti-Obesity Drug? Considerations Based on Primary In Vivo Assays and ADME-Tox Profile In Vitro, Molecules, 24 (2019).

[49] G. Latacz, A. Lubelska, M. Jastrzebska-Wiesek, A. Partyka, M.A. Marc, G. Satala, D. Wilczynska, M. Kotanska, M. Wiecek, K. Kaminska, A. Wesolowska, K. Kiec-Kononowicz, J. Handzlik, The 1,3,5-Triazine Derivatives as Innovative Chemical Family of 5-HT6 Serotonin Receptor Agents with Therapeutic Perspectives for Cognitive Impairment, Int J Mol Sci, 20 (2019).
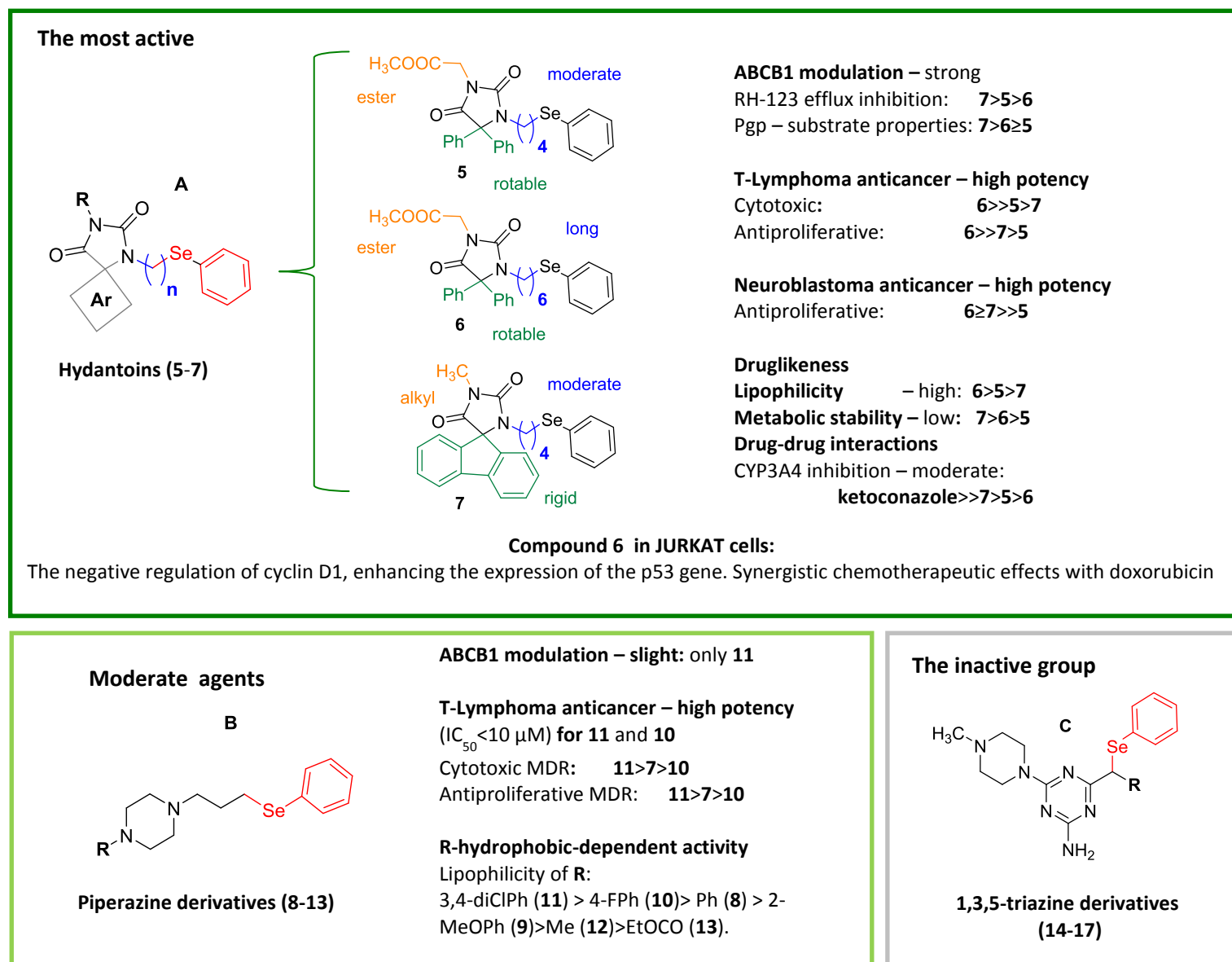
**Figure(s)**



Fig. 10. SAR overview of compounds 5-17. The common phenylselenoether (red) moiety is probably responsible for the trend of more potent antiproliferative activity in the resistant T-Lymphoma (MDR), than that in sensitive (PAR) cells in all three series A-C. Advantage of these new-discovered hydantoin selenoethers (red), referring to previous Se-esters, is the lack of any unpleasant smell and their higher chemical stability

**Supplementary Material - For Publication Online**

**Click here to download Supplementary Material - For Publication Online: corr Supplementary data.pdf**